cerebrum, cerebellum, brainstem, and dorsal root ganglia as well as in nonneuronal tissues such as heart, muscle, and pancreas. Male AR-97Q mice showed markedly more abundant diffuse nuclear staining and NIs than females, in agreement with the symptomatic and Western blot profile differences with gender. Despite the profound sexual difference of the pathogenic AR protein expression, there was no significant difference in the expression of the transgene mRNA between the male and female AR-97Q mice. These observations indicate that the testosterone level plays important roles in the sexual difference of phenotypes, especially in the post-transcriptional stage of the pathogenic AR.

The dramatic sexual difference of phenotypes led us to hormonal interventions in our mouse model. First, we castrated male AR-97Q mice in order to decrease their testosterone level. Castrated male AR-97Q mice showed profound improvement of symptoms, histopathologic findings, and nuclear localization of the pathogenic AR compared with the sham-operated male AR-97Q mice. Body weight, motor function, and lifespan of male AR-97Q mice were significantly improved by castration. Western blot analysis and histopathology revealed diminished nuclear accumulation of the pathogenic AR in the castrated male AR-97Q mice. Next, we administered testosterone to the female AR-97Q mice. In contrast to castration of the male mice, testosterone caused significant aggravation of symptoms, histopathologic features, and nuclear localization of the pathogenic AR in the female AR-97Q mice. Since the nuclear translocation of AR is ligand-dependent, testosterone appears to show toxic effects in the female AR-97Q mice by accelerating nuclear translocation of the pathogenic AR. On the contrary, castration prevented the nuclear localization of the pathogenic AR by reducing the testosterone level. The nuclear accumulation of the pathogenic AR protein with an expanded polyglutamine tract is likely essential in inducing neuronal cell dysfunction and degeneration in the majority of polyglutamine diseases. It thus appears logical that reduction in testosterone level improves phenotypic expression by preventing nuclear localization of the pathogenic AR. In support of this hypothesis, the ligand-dependent neurodegeneration has also been revealed in a fruit fly model of SBMA (Takeyama et al., 2002). Alternatively, castration may enhance protective effects of molecular chaperones, which are normally associated with AR and dissociate upon ligand binding.

Testosterone blockade therapy for SBMA

Successful treatment of AR-97Q mice with castration inspired us testosterone blockade therapies using leuprorelin and flutamide (Katsuno et al., 2003). Leuprorelin is a potent luteinizing hormone-releasing hormone (LHRH) analog suppressing the releases of gonadotrophins, luteinizing hormone and follicle-stimulating hormone. This drug has been used for a variety of sex hormone-dependent diseases including prostate cancer, endometriosis, and prepuberty. The primary pharmacological target of leuprorelin is the anterior pituitary. Through its agonizing effect on LHRH-releasing cells, it initially promotes the releases of gonadotrophins, resulting in transient increase in the serum level of testosterone or estrogens. After this surge, the continued use of this drug induces desensitization of the pituitary by reducing LHRH receptor binding sites and/or uncoupling of receptors from intracellular processes. Within about 2 to 4 weeks of leuprorelin administration, human serum testosterone level decreases to the extent achieved by surgical castration. The effects are maintained during the treatment, suggesting that continuous administration of leuprorelin is required for its clinical use. This drug thus has been provided as sustained release depot taking the form of polymer microspheres. On the other hand, flutamide, the first discovered androgen antagonist, has highly specific affinity for AR and competes with testosterone for binding to the receptor. It has been used for the treatment of prostate cancer, usually in association with an LHRH analog, in order to block the action of adrenal testosterone. Although flutamide suppresses the androgen-dependent transactivation, it does not reduce the plasma levels of testosterone.

Leuprorelin successfully inhibited nuclear accumulation of the pathogenic AR, resulting in marked amelioration of neuromuscular phenotypes seen in the male AR-97Q mice (Fig. 2). Leuprorelin initially increased the serum testosterone level by agonizing the LHRH receptor but subsequently reduced it to undetectable levels. Androgen blockade effects were also confirmed by reduced weights of the prostate and seminal vesicle. The leuprorelin-treated AR-97Q mice showed longer lifespan, larger body size, and better motor performance compared with vehicle-treated mice. Although leuprorelin-induced infertility was prevented by dose reduction, the therapeutic effects on neuromuscular phenotypes were insufficient at a lower dose of leuprorelin. In the Western blot analysis and anti-polyglutamine immunohistochemistry, the leuprorelin-treated male AR-97Q mice demonstrated a markedly diminished amount of the pathogenic AR in the nucleus, suggesting that leuprorelin successfully reduced nuclear AR accumulation. Testosterone, which was given from 13 weeks of age, markedly aggravated neurological symptoms and pathologic findings of leuprorelin-treated male AR-97Q mice. Leuprorelin appears to improve neuronal dysfunction by preventing ligand-dependent nuclear translocation of the pathogenic AR in the same way as castration. Given its minimal invasiveness and established safety, leuprorelin appears to be a promising therapeutic agent for SBMA. In a preliminary open trial, 6-month treatment with leuprorelin significantly diminished nuclear accumulation of pathogenic AR in the scrotal skin of patients, suggesting that androgen deprivation intervenes in the pathogenic process of human SBMA, as demonstrated in animal studies (Banno et al., in press). Another trial on a larger scale is currently underway to verify clinical benefits of leuprorelin for SBMA patients.

Leuprorelin-treated AR-97Q mice showed deterioration of body weight and rotarod task at the age of 8–9 weeks, when serum testosterone initially increased through the agonistic effect of leuprorelin. This change was transient and followed by sustained amelioration along with consequent suppression of testosterone production. The foot print analysis also revealed temporary exacerbation of motor impairment. Immunostaining of tail specimen, sampled from the same individual mouse,

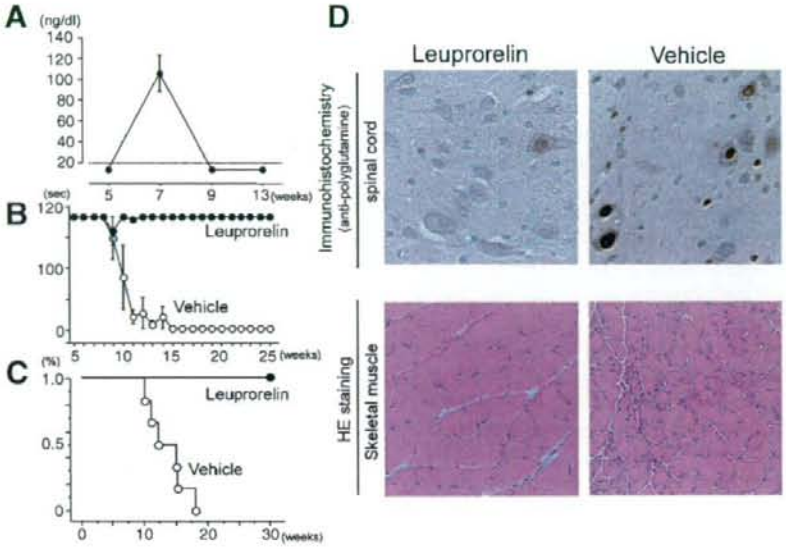

Fig. 2. Effects of leuprorelin on mutant androgen receptor (AR) expression and neuropathology of male AR-97Q mice. (A) Serum testosterone level in AR-97Q mice. Leuprorelin initially increased serum testosterone level but subsequently reduced it to undetectable levels. (B and C) Rotarod task (B) and survival rate (C) of the AR-97Q mice. Leuprorelin markedly improved motor function of the mice at the dose. (D) Immunohistochemistry using 1C2 showed marked differences in diffuse nuclear staining and nuclear inclusions between the leuprorelin-treated and vehicle-treated AR-97Q male mice in the spinal anterior horn. HE staining of the muscle in the vehicle-treated male mouse revealed apparent grouped atrophy and small angulated fibers, which were not seen in the leuprorelin-treated mice.

demonstrated an increase in the number of the muscle fibers with nuclear 1C2 staining at 4 weeks of leuprorelin administration, although this 1C2 staining was diminished by another 4 weeks of treatment. Our results indicate that preventing nuclear translocation of the pathogenic AR is enough to reverse both symptomatic and pathologic phenotypes in our AR-97Q mice. In support with these observations, testosterone deprivation by means of castration reverses motor dysfunction in another transgenic mouse model of SBMA showing fairly slow progression (Chevalier-Larsen et al., 2004). Since the pathophysiology of AR-97Q mice is neuronal dysfunction without neuronal cell loss, our results indicate that the pathogenesis of polyglutamine diseases is reversible at least in its initial stage. From therapeutic point of view, it is of importance to determine the early dysfunctional period in the natural history of human SBMA.

By contrast, flutamide, AR antagonist, did not ameliorate symptoms, pathologic features, or nuclear localization of the pathogenic AR in the male AR-97Q mice, although there was no significant difference in the androgen blockade effects between flutamide and leuprorelin. Flutamide does not inhibit, but may even facilitate, the nuclear translocation of AR. In *consistency* with mouse study, this AR antagonist also promotes nuclear translocation of the pathogenic AR containing an expanded polyglutamine in cellular and fly models of SBMA (Takeyama et al., 2002; Walcott and Merry, 2002). This appears to be the reason why flutamide demonstrated no therapeutic effect in our transgenic mouse model of SBMA. Flutamide is not likely to be a proper therapeutic agent for SBMA.

The castrated or leuprorelin-treated AR-97Q mice showed phenotypes similar to those seen in the female AR-97Q mice, implying that motor impairment of SBMA patients can be reduced to the level in females. SBMA has been considered an X-linked disease, whereas other polyglutamine diseases show autosomal dominant inheritance. In fact, SBMA female patients hardly manifest clinical phenotypes, although they *possess* similar number of a CAG repeat in the disease allele of AR gene as their siblings with SBMA (Sobue et al., 1993; Mariotti et al., 2000). Reduction in the mutant AR expression due to X-inactivation may prevent females from disease manifestation, but hormonal intervention studies using mouse and fly models clearly suggest that low level of testosterone prevents nuclear accumulation of the pathogenic AR protein, resulting in a lack of neurological phenotypes in the females. This view is strongly supported by the observation that manifestation of symptoms is minimal even in homozygous females of SBMA (Schmidt et al., 2002). Therefore, it seems inappropriate to regard SBMA as an X-recessive inherited disease, but rather its neurological phenotype is likely to depend on testosterone concentration.

Role of heat shock proteins in pathogenesis of SBMA

Many components of ubiquitine-proteasome and molecular chaperones are known to colocalize with polyglutamine-containing NIs, implying that failure of cellular defense mechanism underlies neurodegeneration in polyglutamine diseases. Heat shock protein (HSP), a stress-inducible molecular chaperone, is another key to elucidation of the pathogenesis of SBMA. HSPs are classified into different families according to molecular size: Hsp100, Hsp90, Hsp70, Hsp60, Hsp40, and small HSPs (Macario and Conway de Macario, 2005). These HSPs are either constitutively expressed or inducibly

synthesized after cellular stress. HSPs play a crucial role in maintaining correct folding, assembly, and intracellular transport of proteins. For example, Hsp70 and Hsp90, essential components of AR-chaperone complex in the cell cytoplasm, regulate function, nuclear translocation, and degradation of AR (Heinlein and Chang, 2001). Under toxic conditions, HSP synthesis is rapidly upregulated, and nonnative proteins are refolded as a consequence. Therefore, HSPs have attracted a great deal attention as cytoprotective agents against detrimental conditions including ischemia and malignancy.

Several studies suggest that polyglutamine elongation interferes with the protective cellular responses against cytotoxic stress (Wyttenbach, 2004). Truncated AR with an expanded polyglutamine tract delays the induction of Hsp70 after heat shock (Cowan et al., 2003). The threshold of HSP induction is known to be relatively high in spinal motor neurons (Batulan et al., 2003). Expression levels of HSPs are decreased in the brain lesion of an animal model of HD and in that of the SBMA mouse (Hay et al., 2004; Katsuno et al., 2005). Taken together, impairment of HSP induction capability is implicated in the pathogenesis of motor neuron degeneration in SBMA. Not only are HSPs implicated in the pathogenesis of neurodegeneration, but they are also potent suppressors of polyglutamine toxicity. There is increasing evidence that HSPs abrogate polyglutamine-mediated cytotoxicity by refolding and solubilizing the pathogenic proteins (Wyttenbach, 2004; Muchowski and Wacker, 2005). Hsp70 cooperates with Hsp40 in functioning as a molecular chaperone. These HSPs are proposed to prevent the initial conformation conversion of abnormal polyglutamine-containing protein from a random coil to a β-sheet, leading to attenuation of toxic oligomer formation (Wyttenbach, 2004). Overexpression of Hsp70, together with Hsp40, inhibits toxic accumulation of abnormal polyglutamine-containing protein and suppresses cell death in a variety of cellular models of polyglutamine diseases including SBMA (Kobayashi et al., 2000). Hsp70 has also been shown to facilitate proteasomal degradation of abnormal AR protein in a cell culture model of SBMA (Bailey et al., 2002). The favorable effects of Hsp70 have been verified in studies using mouse models of polyglutamine diseases. Overexpression of the inducible form of human Hsp70 markedly ameliorated symptomatic and histopathological phenotypes of our transgenic mouse model of SBMA (Adachi et al., 2003). These beneficial effects are dependent on Hsp70 gene dosage and correlate with the reduction in the amount of nuclear-localized AR protein. It should be noted that the soluble form of the pathogenic AR was also significantly decreased in amount by Hsp70 overexpression, suggesting the degradation of the pathogenic AR may have been accelerated by overexpression of this molecular chaperone.

Favorable effects obtained by genetic modulation of HSP suggest that pharmacological induction of molecular chaperones might be a promising approach to SBMA and other polyglutamine diseases. Geranylgeranylacetone (GGA), an acyclic isoprenoid compound with a retinoid skeleton, has been shown to strongly induce HSP expression in various tissues (Hirakawa et al., 1996). Oral administration of GGA upregulates the levels of Hsp70, Hsp90, and Hsp105 via activation of heat shock factor-1 in the central nervous system and inhibits nuclear accumulation of the pathogenic AR protein, resulting in amelioration of polyglutamine-dependent neuromuscular phenotypes of SBMA transgenic mice (Katsuno et al., 2005). Given its extremely low toxicity, this compound has been used as an oral anti-ulcer drug. Although a high dose appears to be needed for clinical effects, GGA appears to be a safe and promising therapeutic candidate for polyglutamine-mediated neurodegenerative diseases including SBMA.

Inhibition of Hsp90 is also demonstrated to arrest the neurodegeneration in SBMA mouse (Waza et al., 2005). Hsp90 functions in a multi-chaperone complex, assisting proper folding, stabilization, and assembly of so-called client proteins including various oncoproteins and AR (Pratt and Toft, 2003). The Hsp90-client protein complex is stabilized when it is associated with p23, a cochaperone interacting with Hsp90. Treatment with 17-allylamino geldanamycin (17-AAG), a potent Hsp90 inhibitor, dissociated p23 from the Hsp90-AR complex, and thus facilitated proteasomal degradation of the pathogenic AR in cellular and mouse models of SBMA. 17-AAG thereby inhibits nuclear accumulation of this protein, leading to marked amelioration of motor phenotypes of the SBMA mouse model without detectable toxicity (Fig. 3). Of interest is the finding that the pathogenic AR is preferentially targeted to proteasomal degradation in the presence of 17-AAG compared with wild-type AR. Given a high association between p23 and the AR containing expanded polyglutamine, it appears logical that the pathogenic AR is more dependent on Hsp90 to maintain folding and function than wild-type AR and thus is particularly susceptive to Hsp90 inhibition. 17-AAG is also capable of inducing Hsp70 in cellular and mouse models of SBMA. Collectively, 17-AAG, which is now under clinical trials for a wide range of malignancies, would be a good candidate for treatment of SBMA.

Transcriptional dysregulation in SBMA

Disruption of transcriptional machinery has also been hypothesized to underlie the pathogenesis of polyglutamine diseases (Sugars and Rubinsztein, 2003). Gene expression analysis indicates that transcriptional disruption is an early change in the pathogenesis of mouse models of polyglutamine diseases. Transcriptional coactivators such as CBP are sequestrated into the polyglutamine-containing NIs through protein–protein interaction in mouse models and patients with polyQ diseases (Nucifora et al., 2001). Alternatively, the interaction between transcriptional coactivators and soluble pathogenic protein has also been demonstrated in animal models of polyglutamine diseases as well as in postmortem tissues of patients (Steffan et al., 2001). The expression of genes regulated through CBP-mediated transcription is decreased in mouse models of polyglutamine diseases (Sugars and Rubinsztein, 2003). CBP functions as histone acetyltransferase, regulating gene transcription and chromatin structure. It has been indicated that the histone acetyltransferase activity of CBP is suppressed in cellular models of polyglutamine diseases. Taken together, transcriptional dysregulation due to decrease in histone acetylation is likely to

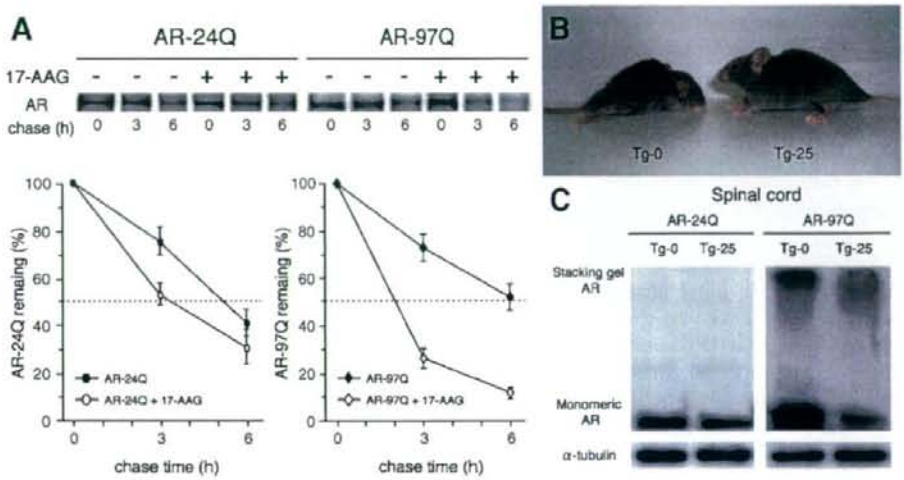

Fig. 3. Effects of 17-AAG on mutant androgen receptor (AR) turnover. (A) Pulse-chase analysis of two forms of AR. The pathogenic AR containing prolonged polyglutamine is degraded more rapidly than the wild-type AR in the presence of 17-AAG. (B) Muscle wasting is obvious in a vehicle-treated SBMA mouse (Tg-0), whereas it is hardly detected in an age-matched SBMA mouse treated with 25 mg/kg of 17-AAG (Tg-25). (C) Western blot analysis of total homogenates from the spinal cord of transgenic mice probed with an anti-AR antibody. 17-AAG decreases the amount of AR in mice bearing the pathogenic AR (AR-97Q), but this effect is only slightly observed in those expressing wild-type AR (AR-24Q).

underlie the pathogenesis of neurodegeneration in polyglutamine diseases. This hypothesis is exemplified by our experimental observation that acetylation of nuclear histone H3 is significantly diminished in SBMA mice (Minamiyama et al., 2004). Additionally, dysfunction of CBP results in a decreased expression of vascular endothelial growth factor in another mouse model of SBMA, indicating the transcriptional alteration is a trigger of neurodegeneration in this disease (Sopher et al., 2004).

Histone acetylation level is determined by interplay between histone acetyltransferase and histone deacetylase (HDAC). Recruitment of HDAC to target genes represses transcription, leading to aberrant cellular function. Since cancellation of

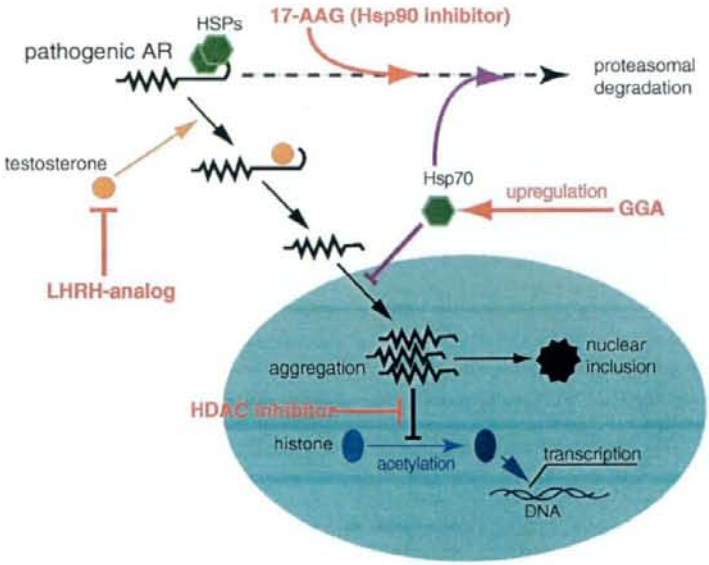

Fig. 4. Pathogenesis-targeting therapeutic approaches to SBMA. In the absence of ligand, the pathogenic AR is confined to a multi-heteromeric inactive complex with heat shock proteins (HSPs) in the cell cytoplasm. Ligand binding facilitates its dissociation from this complex and translocation into the nucleus. In the nucleus, the pathogenic AR forms aggregate and impairs histone acetylation, resulting in transcriptional dysregulation. Several candidates of therapies have been identified on the basis of insights into the molecular mechanisms of the neurodegeneration in SBMA.

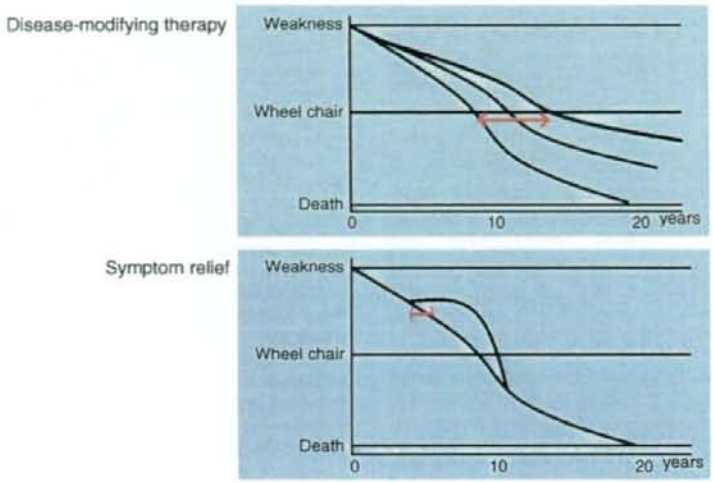

Fig. 5. Disease-modifying therapy and symptom relief. Since the goal of disease-modifying therapy is to inhibit pathogenic progression, long-term trials need to be carried out in order to evaluate drug effects by targeting certain clinical events as the primary endpoint. On the other hand, symptom relief, such as replacement of neurotransmitter, is used to ameliorate symptoms resulting from neurodegeneration. Although trial duration tends to be short, the effect of this therapy is often transient. Arrows indicate trial duration required for each therapy.

HDAC activity results in augmentation of histone acetylation and subsequent restoration of gene transcription, HDAC inhibitors have been considered to be of therapeutic benefit in polyglutamine diseases (Steffan et al., 2001, Hockly et al., 2003). Butyrate is the first HDAC inhibitor to be discovered, and the related compound, phenylbutyrate, has been successfully employed in experimental cancer therapy. Oral administration of sodium butyrate ameliorates symptomatic and histopathological phenotypes of our mouse model of SBMA through upregulation of histone acetylation in nervous tissues (Minamiyama et al., 2004). Although sodium butyrate is likely to be a promising treatment of SBMA, this compound yielded beneficial effects only within a narrow therapeutic window of dosage in the mouse model. Careful dose determination is mandatory when using HDAC inhibitors for treatment of polyglutamine diseases.

Axonal trafficking defects in SBMA

Motor neurons possess extremely long axon along which molecular motors transport essential components such as organelles, vesicles, cytoskeletons, and signal molecules. This implies that axonal trafficking plays a fundamental role in maintenance of normal function of motor neurons. Obstruction of axonal transport has gained attention as a cause of neuronal dysfunction in a variety of neurodegenerative diseases including SBMA (Gunawardena and Goldstein, 2005). A mutation in the gene of proteins regulating axonal trafficking, dynein and dynactin 1, has been shown to cause motor neuron degeneration in both human and rodent (Puls et al., 2003; Hafezparast et al., 2003). Experimental data suggest that axonal transport might be retarded by pathogenic polyglutamine-containing AR (Szebenyi et al., 2003). Although this notion is intriguing, its contribution to the pathogenesis of SBMA should be further investigated, since aggregation of the pathogenic AR is rarely found within the axon of motor neurons in patients or model mice.

Clinical application of potential therapeutics

Analysis of cellular and animal models provides insight into mechanisms involved in neurodegeneration of SBMA and indicates retinal therapeutic approaches to this disease (Fig. 4). Therapeutic agent candidates for SBMA are grossly classified into two groups:

Table 1
Summary of therapeutic trials in SBMA mouse models

Treatment	Number of mice (per treatment group)	Increase in survival (%)	Rotarod task	Body weight	AR accumulation	Reference
Castration	6	>120%	Improved	Improved	Decreased	Katsuno et al. (2002)
Castration[a]	8–9	Not determined	Improved	No effect	Decreased	Chevalier-Larsen et al. (2004)
Leuprorelin	6	>130%	Improved	Improved	Decreased	Katsuno et al. (2003)
Flutamide	6	No effect	No effect	No effect	No effect	Katsuno et al. (2003)
Sodium butyrate	12–15	56%	Improved	Improved	No effect	Minamiyama et al. (2004)
17-AAG	27	>60%	Improved	Improved	Decreased	Waza et al. (2005)
GGA	12–15	>60%	Improved	Improved	Decreased	Katsuno et al. (2005)

[a] Treatment is initiated after the onset of motor impairment. AR, androgen receptor; 17-AAG, 17-allylamino geldanamycin; GGA, geranylgeranylacetone.

(i) drugs inhibiting accumulation of the pathogenic AR protein and (ii) drugs mitigating downstream pathological events including transcriptional dysregulation. The ideal therapy for polyglutamine diseases appears to be a combination of these potential therapeutic strategies, since each drug has potential adverse effects when used in a long term (Agrawal et al., 2005). In addition to pharmacological approaches, genetic interventions such as RNA interference can be applied if safety and delivery problems are solved (Caplen et al., 2002).

Since various therapeutic strategies for SBMA have emerged thanks to animal models recapitulating human diseases, it is of utmost importance to pursue intensive clinical studies to verify the results from animal studies (Table 1). When we apply candidate agents for patients, it should be considered that the majority of therapeutics emerging form animal studies are disease-modifying therapy, but not symptom-relief (Fig. 5). Given that SBMA is a slowly progressive disease, extremely long-term clinical trials are likely necessary to verify clinical benefits of disease-modifying therapies by targeting clinical endpoints such as occurrence of aspiration pneumonia or becoming wheelchair-bound. Suitable surrogate endpoints, which reflect the pathogenesis and severity of SBMA, are thus substantial to assess the therapeutic efficacy in drug trials. To this end, appropriate biomarkers should be identified and validated in translational researches.

Acknowledgments

Fig. 2 is reproduced from Katsuno et al., "Leuprorelin rescues polyglutamine-dependent phenotypes in a transgenic mouse model of spinal and bulbar muscular atrophy (SBMA)" Nat. Med. 9: 768–773, 2003. Fig. 3 is reproduced from Waza et al., "17-AAG, an Hsp90 inhibitor, ameliorates polyglutamine-mediated motor neuron degeneration" Nat. Med. 11: 1088–1095, 2005. This work was supported by a Center-of-Excellence (COE) grant from the Ministry of Education, Culture, Sports, Science and Technology, Japan, and grants from the Ministry of Health, Labour and Welfare, Japan.

References

Adachi, H., Kume, A., Li, M., Nakagomi, Y., Niwa, H., Do, J., Sang, C., Kobayashi, Y., Doyu, M., Sobue, G., 2001. Transgenic mice with an expanded CAG repeat controlled by the human AR promoter show polyglutamine nuclear inclusions and neuronal dysfunction without neuronal cell death. Hum. Mol. Genet. 10, 1039–1048.

Adachi, H., Katsuno, M., Minamiyama, M., Sang, C., Pagoulatos, G., Angelidis, C., Kusakabe, M., Yoshiki, A., Kobayashi, Y., Doyu, M., Sobue, G., 2003. Heat shock protein 70 chaperone overexpression ameliorates phenotypes of the spinal and bulbar muscular atrophy transgenic mouse model by reducing nuclear-localized mutant androgen receptor protein. J. Neurosci. 23, 2203–2211.

Adachi, H., Katsuno, M., Minamiyama, M., Waza, M., Sang, C., Nakagomi, Y., Kobayashi, Y., Tanaka, F., Doyu, M., Inukai, A., Yoshida, M., Hashizume, Y., Sobue, G., 2005. Widespread nuclear and cytoplasmic accumulation of mutant androgen receptor in SBMA patients. Brain 128, 659–670.

Agrawal, N., Pallos, J., Slepko, N., Apostol, B.L., Bodai, L., Chang, L.W., Chiang, A.S., Thompson, L.M., Marsh, J.L., 2005. Identification of combinatorial drug regimens for treatment of Huntington's disease using *Drosophila*. Proc. Natl. Acad. Sci. U. S. A. 102, 3777–3781.

Arrasate, M., Mitra, S., Schweitzer, E.S., Segal, M.R., Finkbeiner, S., 2004. Inclusion body formation reduces levels of mutant huntingtin and the risk of neuronal death. Nature 431, 805–810.

Bailey, C.K., Andriola, I.F., Kampinga, H.H., Merry, D.E., 2002. Molecular chaperones enhance the degradation of expanded polyglutamine repeat androgen receptor in a cellular model of spinal and bulbar muscular atrophy. Hum. Mol. Genet. 11, 515–523.

Banno, H., Adachi, H., Katsuno, M., Suzuki, K., Atsuta, N., Watanabe, H., Tanaka, F., Doyu, M., Sobue, G., in press. Mutant androgen receptor accumulation in SBMA scrotal skin: a pathogenic marker. Ann. Neurol.

Batulan, Z., Shinder, G.A., Minotti, S., He, B.P., Doroudchi, M.M., Nalbantoglu, J., Strong, M.J., Durham, H.D., 2003. High threshold for induction of the stress response in motor neurons is associated with failure to activate HSF1. J. Neurosci. 23, 5789–5798.

Caplen, N.J., Taylor, J.P., Statham, V.S., Tanaka, F., Fire, A., Morgan, R.A., 2002. Rescue of polyglutamine-mediated cytotoxicity by double-stranded RNA-mediated RNA interference. Hum. Mol. Genet. 11, 175–184.

Chevalier-Larsen, E.S., O'Brien, C.J., Wang, H., Jenkins, S.C., Holder, L., Lieberman, A.P., Merry, D.E., 2004. Castration restores function and neurofilament alterations of aged symptomatic males in a transgenic mouse model of spinal and bulbar muscular atrophy. J. Neurosci. 24, 4778–4786.

Clark, P.E., Irvine, R.A., Coetzee, G.A., 2003. The androgen receptor CAG repeat and prostate cancer risk. Methods Mol. Med. 81, 255–266.

Cowan, K.J., Diamond, M.I., Welch, W.J., 2003. Polyglutamine protein aggregation and toxicity are linked to the cellular stress response. Hum. Mol. Genet. 12, 1377–1391.

Doyu, M., Sobue, G., Mukai, E., Kachi, T., Yasuda, T., Mitsuma, T., Takahashi, A., 1992. Severity of X-linked recessive bulbospinal neuronopathy correlates with size of the tandem CAG repeat in androgen receptor gene. Ann. Neurol. 32, 707–710.

Fischbeck, K.H., 1997. Kennedy disease. J. Inherited Metab. Dis. 20, 152–158.

Gatchel, J.R., Zoghbi, H.Y., 2005. Diseases of unstable repeat expansion: mechanism and principles. Nat. Rev., Genet. 6, 743–755.

Gunawardena, S., Goldstein, L.S., 2005. Polyglutamine diseases and transport problems: deadly traffic jams on neuronal highways. Arch. Neurol. 62, 46–51.

Hafezparast, M., Klocke, R., Ruhrberg, C., Marquardt, A., Ahmad-Annuar, A., Bowen, S., Lalli, G., Witherden, A.S., Hummerich, H., Nicholson, S., Morgan, P.J., Oozageer, R., Priestley, J.V., Averillm, S., King, V.R., Ball, S., Peters, J., Toda, T., Yamamoto, A., Hiraoka, Y., Augustin, M., Korthaus, D., Wattler, S., Wabnitz, P., Dickneite, C., Lampel, S., Boehme, F., Peraus, G., Popp, A., Rudelius, M., Schlegel, J., Fuchs, H., Hrabe de Angelis, M., Schiavo, G., Shima, D.T., Russ, A.P., Stumm, G., Martin, J.E., Fisher, E.M., 2003. Mutations in dynein link motor neuron degeneration to defects in retrograde transport. Science 300, 808–812.

Hay, D.G., Sathasivam, K., Tobaben, S., Stahl, B., Marber, M., Mestril, R., Mahal, A., Smith, D.L., Woodman, B., Bates, G.P., 2004. Progressive decrease in chaperone protein levels in a mouse model of Huntington's disease and induction of stress proteins as a therapeutic approach. Hum. Mol. Genet. 13, 1389–1405.

Heinlein, C.A., Chang, C., 2001. Role of chaperones in nuclear translocation and transactivation of steroid receptors. Endocrine 14, 143–149.

Hirakawa, T., Rokutan, K., Nikawa, T., Kishi, K., 1996. Geranylgeranylacetone induces heat shock proteins in cultured guinea pig gastric mucosal cells and rat gastric mucosa. Gastroenterology 111, 345–357.

Hockly, E., Richon, V.M., Woodman, B., Smith, D.L., Zhou, X., Rosa, E., Sathasivam, K., Ghazi-Noori, S., Mahal, A., Lowden, P.A., Steffan, J.S., Marsh, J.L., Thompson, L.M., Lewis, C.M., Marks, P.A., Bates, G.P., 2003. Suberoylanilide hydroxamic acid, a histone deacetylase inhibitor, ameliorates motor deficits in a mouse model of Huntington's disease. Proc. Natl. Acad. Sci. U. S. A. 100, 2041–2046.

Katsuno, M., Adachi, H., Kume, A., Li, M., Nakagomi, Y., Niwa, H., Sang, C., Kobayashi, Y., Doyu, M., Sobue, G., 2002. Testosterone reduction prevents phenotypic expression in a transgenic mouse model of spinal and bulbar muscular atrophy. Neuron 35, 843–854.

Katsuno, M., Adachi, H., Doyu, M., Minamiyama, M., Sang, C., Kobayashi, Y., Inukai, A., Sobue, G., 2003. Leuprorelin rescues polyglutamine-dependent phenotypes in a transgenic mouse model of spinal and bulbar muscular atrophy. Nat. Med. 9, 768–773.

Katsuno, M., Adachi, H., Tanaka, F., Sobue, G., 2004. Spinal and bulbar muscular atrophy: ligand-dependent pathogenesis and therapeutic perspectives. J. Mol. Med. 82, 298–307.

Katsuno, M., Sang, C., Adachi, H., Minamiyama, M., Waza, M., Tanaka, F., Doyu, M., Sobue, G., 2005. Pharmacological induction of heat-shock proteins alleviates polyglutamine-mediated motor neuron disease. Proc. Natl. Acad. Sci. U. S. A. 102, 16801–16806.

Kawahara, H., 1897. A family of progressive bulbar palsy. Aichi. Med. J. 16, 3–4 (in Japanese).

Kennedy, W.R., Alter, M., Sung, J.H., 1968. Progressive proximal spinal and bulbar muscular atrophy of late onset. A sex-linked recessive trait. Neurology 18, 671–680.

Kobayashi, Y., Miwa, S., Merry, D.E., Kume, A., Mei, L., Doyu, M., Sobue, G., 1998. Caspase-3 cleaves the expanded androgen receptor protein of spinal and bulbar muscular atrophy in a polyglutamine repeat length-dependent manner. Biochem. Biophys. Res. Commun. 252, 145–150.

Kobayashi, Y., Kume, A., Li, M., Doyu, M., Hata, M., Ohtsuka, K., Sobue, G., 2000. Chaperones Hsp70 and Hsp40 suppress aggregate formation and apoptosis in cultured neuronal cells expressing truncated androgen receptor protein with expanded polyglutamine tract. J. Biol. Chem. 275, 8772–8778.

La Spada, A.R., Wilson, E.M., Lubahn, D.B., Harding, A.E., Fischbeck, K.H., 1991. Androgen receptor gene mutations in X-linked spinal and bulbar muscular atrophy. Nature 352, 77–79.

Li, M., Miwa, S., Kobayashi, Y., Merry, D.E., Yamamoto, M., Tanaka, F., Doyu, M., Hashizume, Y., Fischbeck, K.H., Sobue, G., 1998. Nuclear inclusions of the androgen receptor protein in spinal and bulbar muscular atrophy. Ann. Neurol. 44, 249–254.

Macario, A.J., Conway de Macario, E., 2005. Sick chaperones, cellular stress, and disease. N. Engl. J. Med. 353, 1489–1501.

Mariotti, C., Castellotti, B., Pareyson, D., Testa, D., Eoli, M., Antozzi, C., Silani, V., Marconi, R., Tezzon, F., Siciliano, G., Marchini, C., Gellera, C., Donato, S.D., 2000. Phenotypic manifestations associated with CAG-repeat expansion in the androgen receptor gene in male patients and heterozygous females: a clinical and molecular study of 30 families. Neuromuscul. Disord. 10, 391–397.

Minamiyama, M., Katsuno, M., Adachi, H., Waza, M., Sang, C., Kobayashi, Y., Tanaka, F., Doyu, M., Inukai, A., Sobue, G., 2004. Sodium butyrate ameliorates phenotypic expression in a transgenic mouse model of spinal and bulbar muscular atrophy. Hum. Mol. Genet. 13, 1183–1192.

Muchowski, P.J., Wacker, J.L., 2005. Modulation of neurodegeneration by molecular chaperones. Nat. Rev., Neurosci. 6, 11–22.

Nucifora Jr., F.C., Sasaki, M., Peters, M.F., Huang, H., Cooper, J.K., Yamada, M., Takahashi, H., Tsuji, S., Troncoso, J., Dawson, V.L., Dawson, T.M., Ross, C.A., 2001. Interference by huntingtin and atrophin-1 with cbp-mediated transcription leading to cellular toxicity. Science 291, 2423–2428.

Poletti, A., 2004. The polyglutamine tract of androgen receptor: from functions to dysfunctions in motor neurons. Front. Neuroendocrinol. 25, 1–26.

Pratt, W.B., Toft, D.O., 2003. Regulation of signaling protein function and trafficking by the hsp90/hsp70-based chaperone machinery. Exp. Biol. Med. 228, 111–133.

Puls, I., Jonnakuty, C., LaMonte, B.H., Holzbaur, E.L., Tokito, M., Mann, E., Floeter, M.K., Bidus, K., Drayna, D., Oh, S.J., Brown Jr., R.H., Ludlow, C.L., Fischbeck, K.H., 2003. Mutant dynactin in motor neuron disease. Nat. Genet. 33, 455–456.

Schmidt, B.J., Greenberg, C.R., Allingham-Hawkins, D.J., Spriggs, E.L., 2002. Expression of X-linked bulbospinal muscular atrophy (Kennedy disease) in two homozygous women. Neurology 59, 770–772.

Sobue, G., Hashizume, Y., Mukai, E., Hirayama, M., Mitsuma, T., Takahashi, A., 1989. X-linked recessive bulbospinal neuronopathy. A clinicopathological study. Brain 112, 209–232.

Sobue, G., Doyu, M., Kachi, T., Yasuda, T., Mukai, E., Kumagai, T., Mitsuma, T., 1993. Subclinical phenotypic expressions in heterozygous females of X-linked recessive bulbospinal neuronopathy. J. Neurol. Sci. 117, 74–78.

Sopher, B.L., Thomas, Jr., P.S., LaFevre-Bernt, M.A., Holm, I.E., Wilke, S.A., Ware, C.B., Jin, L.W., Libby, R.T., Ellerby, L.M., La Spada, A.R., 2004. Androgen receptor YAC transgenic mice recapitulate SBMA motor neuronopathy and implicate VEGF164 in the motor neuron degeneration. Neuron 41, 687–699.

Sperfeld, A.D., Karitzky, J., Brummer, D., Schreiber, H., Haussler, J., Ludolph, A.C., Hanemann, C.O., 2002. X-linked bulbospinal neuropathy: Kennedy disease. Arch. Neurol. 59, 1921–1926.

Steffan, J.S., Bodai, L., Pallos, J., Poelman, M., McCampbell, A., Apostol, B.L., Kazantsev, A., Schmidt, E., Zhu, Y.Z., Greenwald, M., Kurokawa, R., Housman, D.E., Jackson, G.R., Marsh, J.L., Thompson, L.M., 2001. Histone deacetylase inhibitors arrest polyglutamine-dependent neurodegeneration in *Drosophila*. Nature 413, 739–743.

Sugars, K.L., Rubinsztein, D.C., 2003. Transcriptional abnormalities in Huntington disease. Trends Genet. 19, 233–238.

Szebenyi, G., Morfini, G.A., Babcock, A., Gould, M., Selkoe, K., Stenoien, D.L., Young, M., Faber, P.W., MacDonald, M.E., McPhaul, M.J., Brady, S.T., 2003. Neuropathogenic forms of huntingtin and androgen receptor inhibit fast axonal transport. Neuron 40, 41–52.

Takeyama, K., Ito, S., Yamamoto, A., Tanimoto, H., Furutani, T., Kanuka, H., Miura, M., Tabata, T., Kato, S., 2002. Androgen-dependent neurodegeneration by polyglutamine-expanded human androgen receptor in *Drosophila*. Neuron 35, 855–864.

Walcott, J.L., Merry, D.E., 2002. Ligand promotes intranuclear inclusions in a novel cell model of spinal and bulbar muscular atrophy. J. Biol. Chem. 277, 50855–50859.

Waza, M., Adachi, H., Katsuno, M., Minamiyama, M., Sang, C., Tanaka, F., Inukai, A., Doyu, M., Sobue, G., 2005. 17-AAG, an Hsp90 inhibitor, ameliorates polyglutamine-mediated motor neuron degeneration. Nat. Med. 11, 1088–1095.

Wyttenbach, A., 2004. Role of heat shock proteins during polyglutamine neurodegeneration: mechanisms and hypothesis. J. Mol. Neurosci. 23, 69–96.

Mutant Androgen Receptor Accumulation in Spinal and Bulbar Muscular Atrophy Scrotal Skin: A Pathogenic Marker

Haruhiko Banno, MD, Hiroaki Adachi, MD, Masahisa Katsuno, MD, Keisuke Suzuki, MD, Naoki Atsuta, MD, Hirohisa Watanabe, MD, Fumiaki Tanaka, MD, Manabu Doyu, MD, and Gen Sobue, MD

Objective: **Spinal and bulbar muscular atrophy (SBMA) is a hereditary motor neuron disease caused by the expansion of a polyglutamine tract in the androgen receptor (AR). The nuclear accumulation of mutant AR is central to the pathogenesis of SBMA. Androgen deprivation with leuprorelin inhibits mutant AR accumulation, resulting in rescue of neuronal dysfunction in a mouse model of SBMA. This study aimed to investigate whether mutant AR accumulation in the scrotal skin is an appropriate biomarker of SBMA.** ***Methods:*** **Immunohistochemistry of both scrotal skin and the spinal cord was performed on five autopsied SBMA cases. Neurological severity and scrotal skin findings were studied in another 13 patients. Five other patients received subcutaneous injections of leuprorelin and underwent scrotal skin biopsy.** ***Results:*** **The degree of mutant AR accumulation in scrotal skin epithelial cells tended to be correlated with that in the spinal motor neurons in autopsy specimens, and it was well correlated with CAG repeat length and inversely correlated with the amyotrophic lateral sclerosis functional scale. Leuprorelin treatment inhibited mutant AR protein accumulation in the scrotal skin of SBMA patients.** ***Interpretation:*** **These observations suggest that scrotal skin biopsy findings are a potent pathogenic marker of SBMA and can be a surrogate end point in therapeutic trials.**

Ann Neurol 2006;59:520–526

Spinal and bulbar muscular atrophy (SBMA), also known as Kennedy's disease, is an adult-onset motor neuron disease characterized by muscle atrophy, weakness, contraction fasciculations, and bulbar involvement.[1–4] SBMA exclusively affects men in their 30s or 40s, and disease progression is slow.[1,5] The molecular basis of SBMA is the expansion of a trinucleotide CAG repeat, which encodes a polyglutamine (polyQ) tract, in the androgen receptor (AR) gene.[6] The CAG repeat numbers range from 38 to 62 in SBMA patients, whereas healthy individuals have 10 to 36 CAGs.[6,7] The number of CAGs is correlated with disease severity and is inversely correlated with age of onset,[8,9] as observed in other polyQ-related neurodegenerative diseases including Huntington's disease and several forms of spinocerebellar ataxia.[10]

Histopathologically, lower motor neurons are markedly depleted in the spinal cord and brainstem, and nuclear inclusions (NIs) containing the mutant and truncated AR with expanded polyQ are present in the residual motor neurons, as well as in cells of the scrotal skin and other visceral organs.[3,11,12] Although NIs are a disease-specific pathological marker, they may reflect a cellular protective response against the toxicity of abnormal polyQ-containing protein.[13] In contrast, the therapeutic effect of testosterone deprivation in our SBMA transgenic mouse model suggested that diffuse nuclear accumulation of mutant AR is a cardinal pathogenic process underlying neurological manifestations.[14,15] This hypothesis has also been clearly illustrated by the observation that the extent of diffuse nuclear accumulation of mutant AR, but not NIs, in the motor neurons of the spinal cord was closely related to CAG repeat length in autopsied SBMA cases.[16] Nuclear localization of the mutant protein has now been considered essential for inducing neuronal cell dysfunction and degeneration in the majority of polyQ diseases.[10]

A characteristic clinical feature of SBMA is that the disease occurs in male but not female individuals, even when they are homozygous for the mutation.[17,18] Several studies have clarified that the sex dependency of disease manifestation in SBMA arises from testosterone-dependent nuclear accumulation of mu-

From the Department of Neurology, Nagoya University Graduate School of Medicine, Showa-ku, Nagoya, Japan.

Received Sep 1, 2005, and in revised form Oct 4. Accepted for publication Oct 6, 2005.

Published online Dec 15, 2005 in Wiley InterScience (www.interscience.wiley.com). DOI: 10.1002/ana.20735

Address correspondence to Dr Sobue, Department of Neurology, Nagoya University Graduate School of Medicine, 65 Tsurumai-cho, Showa-ku, Nagoya 466-8550, Japan.
E-mail: sobueg@med.nagoya-u.ac.jp

 © 2005 American Neurological Association
Published by Wiley-Liss, Inc., through Wiley Subscription Services

tant AR.[14,15,19,20] Leuprorelin, a leuteinizing hormone–releasing hormone agonist that reduces testosterone release from the testis and inhibits nuclear accumulation of mutant AR, rescued motor dysfunction in male transgenic mice carrying the full-length human AR with expanded polyQ.[15]

Although data from transgenic mice studies indicated that androgen deprivation from leuprorelin treatment is a potent therapeutic agent for SBMA,[14,15] clinical experience using this drug for SBMA patients is limited.[21] Because long-term clinical trials are needed to establish the efficacy of therapeutics ameliorating disease progression in slowly progressive neurodegenerative diseases such as SBMA, an appropriate biomarker reflecting pathogenic processes of the disease is necessary. The aim of this study was to test the hypothesis that peripheral accumulation of mutant AR in the scrotal skin represents a suitable biomarker of SBMA that can be applicable as a surrogate end point in therapeutic trials.

Patients and Methods

Patients

Twenty-three patients with clinically and genetically confirmed SBMA were examined. Patient characteristics are shown in the Table. Five of the 23 patients underwent autopsy, and both the scrotal skin and the spinal cord were examined; another 13 patients underwent biopsy of the scrotal skin. The remaining five patients were enrolled in a leuprorelin study and also underwent biopsy of the scrotal skin. All patients were hospitalized and underwent follow-up examinations at Nagoya University Hospital (Nagoya, Japan) and its affiliated hospitals.

For each of the 18 patients who underwent biopsy of the scrotal skin, three scrotal skin specimens were made by punch biopsy using a 3mm diameter Dermapunch (Nipro, Tokyo, Japan) under 10ml lidocaine acetate local anesthesia. All patients who underwent biopsy sterilized the wound for several days by themselves and received 4 days of cefaclor (250mg three times a day) antibiotic therapy after the procedure. The 13 patients who underwent biopsy who were not enrolled in the leuprorelin trial were also assessed on the amyotrophic lateral sclerosis functional scale (limb Norris score), as described previously.[22]

Five other male subjects (age, 60–74 years; mean, 67.3 years) who died of nonneurological diseases served as control subjects. The Nagoya University Hospital Institutional Review Board approved the collection of data and specimens, and all patients gave their written, informed consent to participate.

Leuprorelin Administration

Five patients received subcutaneous injections of 3.75mg leuprorelin once every 4 weeks. The patients, aged 43 to 68 years, were capable of walking with or without a cane and expressed no desire to father a child. They were observed for 6 months (24 weeks), and scrotal skin biopsies were taken from each patient at 0, 4, and 12 weeks after initial leuprorelin administration. Serum creatine kinase (CK) was determined by ultraviolet measurement using hexokinase and glucose-6-phosphate. Serum testosterone levels were measured by radioimmunoassay using the DPC total testosterone kit (Diagnostic Products Corporation, Los Angeles, CA).

Immunohistochemical Detection of the Mutant Androgen Receptor in the Scrotal Skin and Spinal Cord

Immunohistochemistry of scrotal skin specimens and the spinal cord were conducted as described previously.[16] In brief, we prepared 5μm-thick, formalin-fixed, paraffin-embedded sections of scrotal skin and spinal cord from SBMA patients. Sections were deparaffinized and rehydrated through a graded series of alcohol-water solutions. For the mutant AR immunohistochemical study, sections were pretreated with immersion in 98% formic acid for 5 minutes, and then with microwave oven heating for 15 minutes in 10mM citrate buffer at pH 6.0. Sections were incubated with a mouse anti-expanded polyQ antibody (1:20,000; 1C2; Chemicon, Temecula, CA)[23] to evaluate the nuclear accumulation of mutant AR.[14–16] Immune complexes were visualized using the Envision-plus kit (Dako, Glostrup, Denmark). Sections were counterstained with Mayer's hematoxylin. For electron microscopic immunohistochemistry, the sections were processed

Table. Patient Characteristics

Characteristics	Autopsy Study (N = 5)	Biopsy Alone Study (N = 13)	Leuprorelin + Biopsy Study (N = 5)
Age (mean ± SD), yr	64.8 ± 10.8	54.8 ± 9.6	50.2 ± 10.8
Duration of weakness (mean ± SD), yr	38.4 ± 14.7	11.0 ± 7.4	8.8 ± 4.9
(CAG)n (mean ± SD)	47.4 ± 4.9	48.2 ± 3.0	49.2 ± 4.9
ADL (cane/independent ratio)	NA	4/9	2/3
Limb Norris score (mean ± SD)	NA	53.4 ± 6.9	52.0 ± 6.8
Norris bulbar score (mean ± SD)	NA	32.2 ± 3.4	32.8 ± 6.2
ALSFRS-R (Japanese edition) (mean ± SD)	NA	40.3 ± 3.2	39.2 ± 3.8
Cause of death	Pneumonia (n = 4); Lung cancer (n = 1)	NA	NA

The amyotrophic lateral sclerosis functional rating scale-revised.
SD = standard deviation; (CAG)n = number of expanded CAG repeats in the SBMA allele; NA = not applicable; ADL = activities of daily living.

as described for light microscopic immunohistochemistry, and then fixed with 2% osmium tetroxide in 0.1M phosphate buffer at pH 7.4, dehydrated in graded alcohol-water solutions, and embedded in epoxy resin. Ultrathin sections were cut for observation under an electron microscope (H-7100; Hitachi High-Technologies Corporation, Tokyo, Japan).

Quantification of Cell Population with Diffuse Nuclear Staining

For quantitative assessment of scrotal skin cells, the frequency of diffuse nuclear staining was calculated from counts of more than 500 nuclei in 5 randomly selected fields of each section photographed at 400× magnification (BX51TF; Olympus, Tokyo, Japan). To assess the nuclear accumulation of mutant AR in spinal cord motor neurons, we prepared at least 100 transverse sections each from the cervical, thoracic, and lumber spinal cord for anti-expanded polyQ antibody staining with 1C2. The numbers of 1C2-positive cells in the ventral horn on both the right and left sides were counted on every 10th section under the light microscope with a computer-assisted image analyzer (BX51TF; Olympus), as described previously.[16,24] Populations of 1C2-positive cells were expressed as percentages of the total skin cell or neuronal count.

Statistical Analysis

We analyzed the data by Pearson's coefficient, Spearman's rank correlation, and Student's paired t test as appropriate using StatView software (version 5; Hulinks, Tokyo, Japan) and considering p values less than 0.05 to be indicative of significance.

Results

Mutant Androgen Receptor Nuclear Accumulation in the Scrotal Skin and Spinal Motor Neuron

In the five autopsied cases, mutant AR nuclear accumulations were clearly visualized with anti-expanded polyQ immunostaining with 1C2 in the scrotal skin and spinal cord specimens (Fig 1A). Pathological accumulation of mutant AR was distributed in all layers of the epithelium. Diffuse nuclear accumulations were predominantly observed, and the occurrence of NIs was less frequent. This was also the case in the spinal cord specimens. Electron microscopic immunohistochemistry with the 1C2 antibody demonstrated granular dense and amorphous aggregates corresponding to diffuse nuclear staining in both spinal motor neurons and epithelial cells of scrotal skin (see Figs 1B, C). Filamentous structures such as those reported in Huntington's disease,[25] dentatorubal-pallidoluysian atrophy (DRPLA),[26] and Machado–Joseph disease[27] were not seen. No diffuse nuclear staining was seen in the control subjects. The extent of mutant AR accumulation in the scrotal skin epithelial cells showed a tendency to correlate with that in the anterior horn cells ($r = 0.84$; $p = 0.08$; see Fig 1D). Mutant AR accumulation was remarkable in both the spinal motor neurons and the scrotal skin of Patient 1, but was far less remarkable in Patient 2 (see Figs 1A, D).

Correlations of the Mutant Androgen Receptor Accumulation in the Scrotal Skin to CAG Repeat Length and Amyotrophic Lateral Sclerosis Score

Mutant AR nuclear accumulations in scrotal skin biopsies from the 13 SBMA patients who did not receive leuprorelin were assessed by 1C2 antibody staining of expanded PolyQ. The 1C2-positive cell population in the scrotal skin biopsies was significantly correlated with CAG repeat length ($r = 0.61$; $p = 0.03$; Fig 2A) and was inversely correlated with the functional scale assessed by the Norris score on limbs ($r = -0.63$; $p = 0.02$; see Fig 2B).

Leuprorelin Treatment Depletes Mutant Androgen Receptor Accumulation in the Scrotal Skin

In all five patients in which leuprorelin was administered (see the Table), both the intensity and the frequency of diffuse nuclear 1C2 staining in the scrotal epithelial cells was decreased after the first 4 weeks of administration compared with the preadministration values, and this effect was markedly enhanced after 12 weeks of treatment (Figs 3A, B). Quantitative analysis demonstrated a significant decrease in the frequency of 1C2-positive cells both 4 and 12 weeks after the initiation of leuprorelin treatment ($p < 0.01$) (see Fig 3C). Serum testosterone levels decreased to the castration level after 1 to 2 months of treatment (see Fig 3D), and serum CK values were also significantly decreased in all patients (see Fig 3D).

None of the patients showed the hot flush or obesity often reported in leuprorelin trials for prostate cancer. Although a loss of sexual function including erectile disorder was observed in all patients, no patients experienced depression. No marked exacerbations were observed in total cholesterol, triglyceride, fasting blood sugar, or HbA1c (data not shown). We could not find significant motor function changes assessed by amyotrophic lateral sclerosis functional scores in 24 weeks, but three of the five enrolled patients expressed apparent subjective improvement.

Discussion

This study demonstrated that scrotal skin biopsy with anti-expanded polyQ staining is a strong candidate for an appropriate biomarker with which to monitor SBMA pathogenic processes. Previous studies showed that the severity and progression of motor dysfunction and abatement of abnormalities in mice that were castrated or given leuprorelin paralleled the extent of diffuse nuclear mutant AR accumulation in their spinal motor neurons.[14,15] Furthermore, we demonstrated previously a significant, close correlation between the length of CAG repeat expansion and frequency of dif-

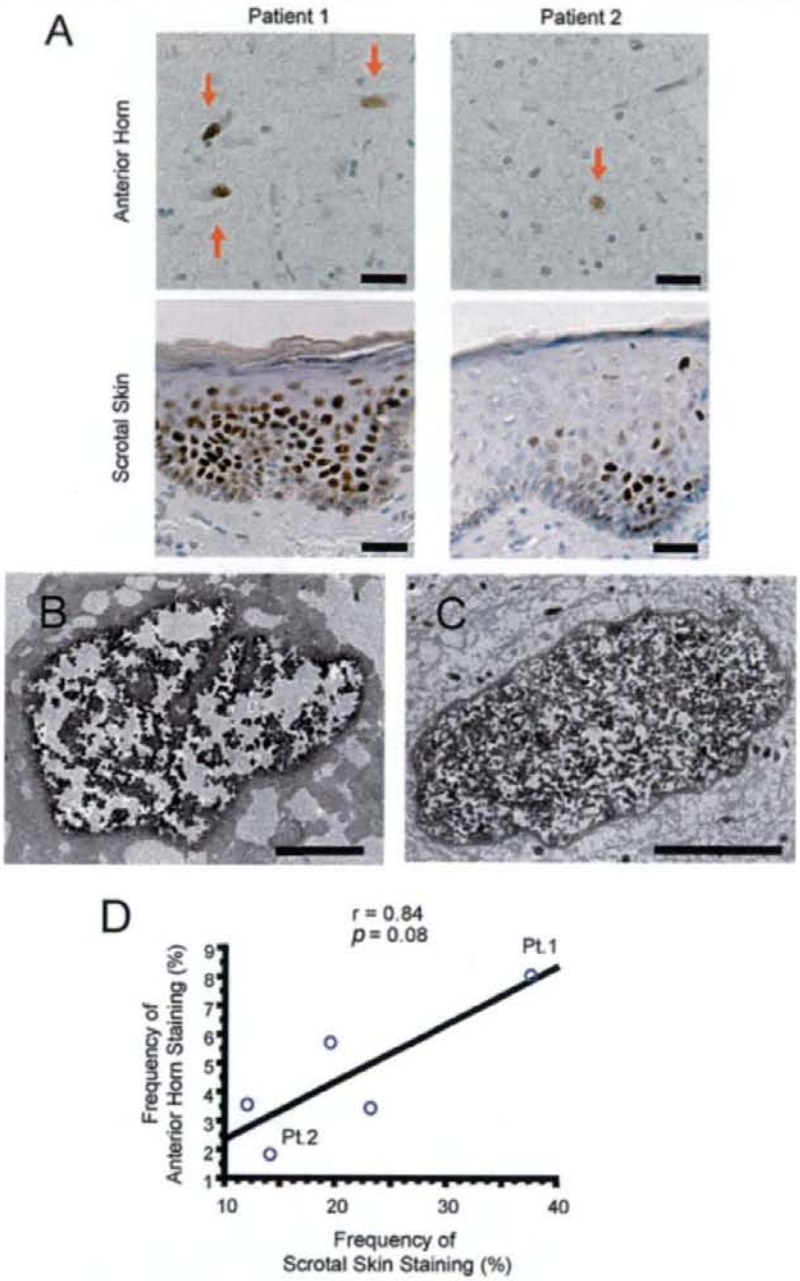

Fig 1. Mutant androgen receptor (AR) nuclear accumulation in scrotal skin and spinal motor neurons. (A) Mutant AR accumulation was remarkable in both spinal motor neurons (arrows) and scrotal skin of Patient 1, but was less remarkable in both motor neurons (arrows) and skin in Patient 2. Bar = 30μm. (B, C) Electron microscopic immunohistochemistry for 1C2 demonstrated granular dense and amorphous aggregates corresponding to diffuse nuclear staining in both spinal motor neurons and epithelial cells of scrotal skin. Bar =3μm. (D) The extent of mutant AR accumulation in scrotal skin epithelial cells showed a tendency to correlate with that in anterior horn cells. Circles (Pt. 1, Pt. 2) correspond to Patient 1 and 2 in Fig 1A.

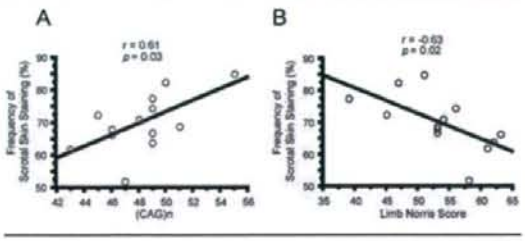

Fig 2. Correlation of the frequency of scrotal skin staining to CAG repeats and limb Norris score. The frequency of 1C2-positive cells in the scrotal skin biopsies correlated significantly with (A) CAG repeat length and (B) inversely correlated with the amyotrophic lateral sclerosis functional scale assessed by the Norris score on limbs. (CAG)n = number of expanded CAG repeats in the spinal and bulbar muscular atrophy allele.

fuse nuclear mutant AR accumulation, but not that of NIs, in the spinal cord.[16] Accordingly, neuronal dysfunction is likely to be caused by diffuse nuclear accumulation of mutant AR in the affected tissues. In this study, the extent of mutant AR nuclear accumulation in scrotal skin cells paralleled that in the anterior horn cells in autopsied cases. Electron microscopic immunohistochemistry for 1C2 anti-expanded PolyQ demonstrated granular dense and amorphous aggregates corresponding to diffuse nuclear staining in both spinal motor neurons and epithelial cells of scrotal skin. Furthermore, the fine structure of the aggregates in spinal motor neurons and epithelial cells was quite similar. Biopsy analyses in this study also suggested that scrotal skin findings were correlated with the motor functional scores of SBMA patients.

Our findings suggest that nuclear mutant AR assessed by 1C2 immunostaining in the scrotal skin is a practical procedure to estimate the severity of SBMA pathogenesis in the nervous system. In support of this view, decreases in mutant AR accumulation in the motor neurons paralleled that in nonneuronal cells in the androgen deprivation therapy tested in the mouse model of SBMA. In addition, leuprorelin treatment markedly reduced serum testosterone levels, as well as nuclear accumulation of mutant AR in the scrotal skin, suggesting that medical castration with leuprorelin intervenes in the pathogenic process of human SBMA, as demonstrated in the animal study. Moreover, serum CK levels were significantly decreased in this leuprorelin study. Because high CK values are common in SBMA patients and histopathological examinations have shown myogenic changes together with neurogenic findings in this disease,[1,3] presumably, a decrease in CK values with leuprorelin treatment implies muscular protection. Serum CK levels, however, did not significantly correlate with the Norris score on limbs or with scrotal skin biopsy findings in our cross-sectional study.

As defined by the Biomarkers Definitions Working Group, a disease biomarker should be objectively measurable and evaluated as an indicator of pathogenic processes or pharmacological responses to a therapeutic intervention.[28] Based on the observations described earlier, 1C2-stained mutant AR accumulation in the biopsied scrotal skin is likely to be a potent biomarker reflecting pathogenic processes of SBMA. Particularly, the correlation of the extent of mutant AR nuclear accumulation in the spinal motor neurons with that in scrotal skin biopsies in the autopsied cases suggests that findings in the scrotal skin can predict pathogenic processes in the motor neurons.

Although its precise natural history has not been evaluated, SBMA is a slowly progressive disease.[1,5] Thus, extremely long-term clinical trials are necessary to assess whether certain drugs can alter the natural disease progression by targeting clinical end points such as occurrence of aspiration pneumonia or becoming wheelchair bound. Suitable surrogate end points, which reflect the pathogenesis and severity of SBMA, are substantial to assess the therapeutic efficacy in drug trials. Although it is not practical to obtain biopsy specimens from the central nervous system (CNS), a punch biopsy of the scrotal skin enables a safe and accessible examination for patients.

It has also been suggested that reliance on surrogate end points can be misleading because they may not accurately predict the actual effects that treatments have on the health of a patient, as was seen with the CD4 counts in human immunodeficiency virus trials, the bone mineral density in osteoporosis trials, and others.[29] However, several factors have been suggested to consider the decision to rely on a surrogate.[30] In SBMA, mutant AR accumulation assessed by scrotal skin biopsy can be a candidate for a surrogate end point in light of several pieces of evidence. First, a credible SBMA animal model demonstrated dramatic functional motor recovery in response to testosterone deprivation therapy that depleted mutant AR accumulation in the central nervous system, as well as in nonneuronal tissues.[14,15] Second, the degree of diffuse nuclear accumulation of mutant AR in both the CNS and scrotal skin correlates well with CAG repeat length and disease severity, indicating that it is a natural phenomenon of and reflects the underlying pathology of the disease. Third, autopsy studies show that levels of nuclear AR accumulation in the scrotal skin are correlated with those in the CNS. Moreover, levels of nuclear translocated mutant AR in the scrotal skin decreased significantly in response to drug therapy that has been shown to deplete such accumulations in the CNS of SBMA mice, to significantly rescue motor dysfunction in these mice, and to partially stabilize neurological symptoms in one reported case of human SBMA.[21]

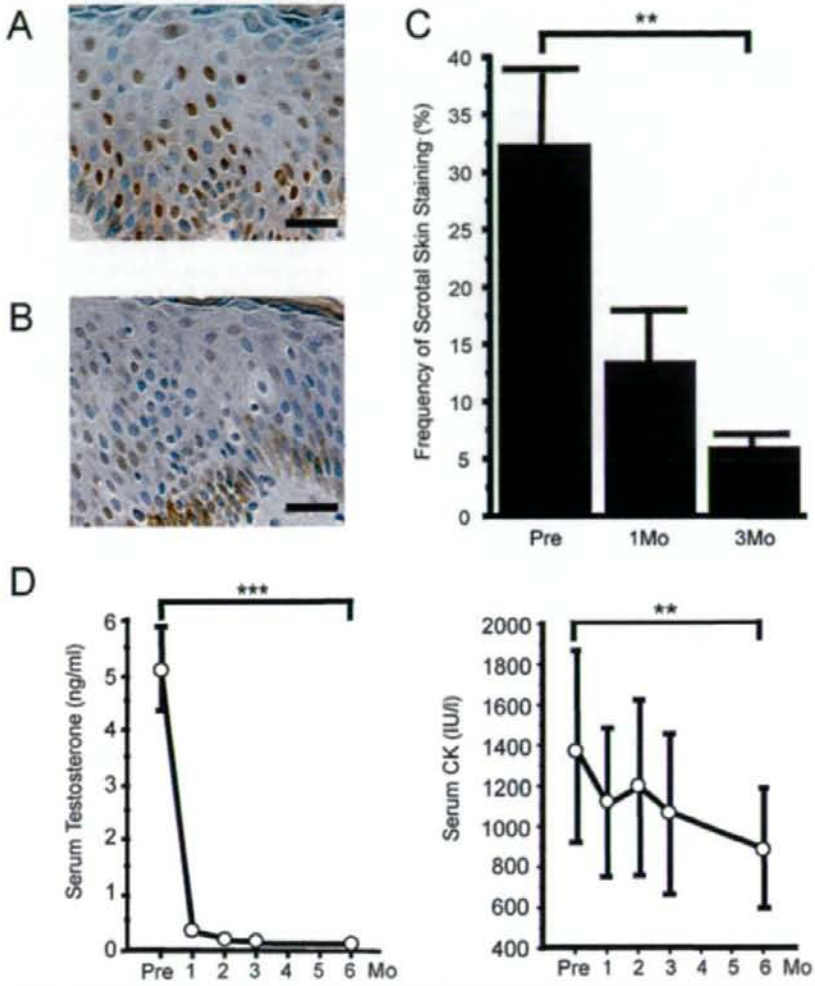

Fig 3. Effects of leuprorelin on mutant androgen receptor (AR) accumulation in scrotal skin, serum testosterone, and creatine kinase (CK). (A) Scrotal skin shows intense and frequent staining for anti-polyglutamine antibody in the nucleus before therapy. (B) Twelve weeks after therapy, both intensity and frequency of nuclear staining markedly decreased. Bar = 30μm. (C) Quantitative analysis of immunohistochemistry demonstrated a significant decrease in the number of positively stained nuclei. (D) Serum testosterone and CK decreased significantly in 6 months. Frequency of staining was calculated from counts of more than 500 nuclei in randomly selected areas and was expressed as mean ± standard deviation for 5 patients. $^{**}p < 0.01$; $^{***}p < 0.0001$.

Although our results were obtained from a small sample, nuclear accumulation of mutant AR in the scrotal skin appears to be a potent pathogenic biomarker of SBMA. A correlation between decline in validated clinical scales and nuclear mutant AR accumulations must be demonstrated in a longitudinal study to verify this histopathological feature as a biomarker for clinical severity. Similarly, validation of the scrotal skin biopsy findings as a surrogate end point in clinical trials will require a longitudinal study verifying that suppression of nuclear staining correlates with improvement on a validated clinical scale and the true clinical outcome events such as the need for a wheelchair, the presence of aspiration pneumonia, or death.

This work was supported by grants from the Ministry of Education, Culture, Sports, Science and Technology, Japan (17204032, G. S., M. D., F. T.); the Ministry of Health, Labor and Welfare, Japan (H-15-Kokoro-020, G. S., M. D.); and the Center for Clinical Trials, Japan Medical Association (G.S.).

We thank Dr N. Hishikawa for technical assistance.

References

1. Kennedy WR, Alter M, Sung JH. Progressive proximal spinal and bulbar muscular atrophy of late onset: a sex-linked recessive trait. Neurology 1968;18:671–680.
2. Sperfeld AD, Karitzky J, Brummer D, et al. X-linked bulbospinal neuropathy: Kennedy disease. Arch Neurol 2002;59: 1921–1926.
3. Sobue G, Hashizume Y, Mukai E, et al. X-linked recessive bulbospinal neuronopathy: a clinicopathological study. Brain 1989; 112:209–232.
4. Katsuno M, Adachi H, Tanaka F, et al. Spinal and bulbar muscular atrophy (SBMA): ligand-dependent pathogenesis and therapeutic perspective. J Mol Med 2004;82:298–307.
5. Sobue G, Adachi H, Katsuno M. Spinal and bulbar muscular atrophy (SBMA). In: Dickinson D, ed. Neurodegeneration: the molecular pathology of dementia and movement disorders. Basel: INS Neuropathology, 2003:275–279.
6. La Spada AR, Wilson EM, Lubahn DB, et al. Androgen receptor gene mutations in X-linked spinal and bulbar muscular atrophy. Nature 1991;352:77–79.
7. Tanaka F, Doyu M, Ito Y, et al. Founder effect in spinal and bulbar muscular atrophy (SBMA). Hum Mol Genet 1996;5: 1253–1257.
8. Doyu M, Sobue G, Mukai E, et al. Severity of X-linked recessive bulbospinal neuronopathy correlates with size of the tandem CAG repeat in androgen receptor gene. Ann Neurol 1992; 32:707–710.
9. Shimada N, Sobue G, Doyu M, et al. X-linked recessive bulbospinal neuronopathy: clinical phenotypes and CAG repeat size in androgen receptor gene. Muscle Nerve 1995;18: 1378–1384.
10. Zoghbi HY, Orr HT. Glutamine repeats and neurodegeneration. Annu Rev Neurosci 2000;23:217–247.
11. Li M, Miwa S, Kobayashi Y, et al. Nuclear inclusions of the androgen receptor protein in spinal and bulbar muscular atrophy. Ann Neurol 1998;44:249–254.
12. Li M, Nakagomi Y, Kobayashi Y, et al. Nonneural nuclear inclusions of androgen receptor protein in spinal and bulbar muscular atrophy. Am J Pathol 1998;153:695–701.
13. Arrasate M, Mitra S, Schweitzer ES, et al. Inclusion body formation reduces levels of mutant huntingtin and the risk of neuronal death. Nature 2004;431:805–810.
14. Katsuno M, Adachi H, Kume A, et al. Testosterone reduction prevents phenotypic expression in a transgenic mouse model of spinal and bulbar muscular atrophy. Neuron 2002;35: 843–854.
15. Katsuno M, Adachi H, Doyu M, et al. Leuprorelin rescues polyglutamine-dependent phenotypes in a transgenic mouse model of spinal and bulbar muscular atrophy. Nat Med 2003; 9:768–773.
16. Adachi H, Katsuno M, Minamiyama M, et al. Widespread nuclear and cytoplasmic accumulation of mutant androgen receptor in SBMA patients. Brain 2005;128:659–670.
17. Sobue G, Doyu M, Kachi T, et al. Subclinical phenotypic expressions in heterozygous females of X-linked recessive bulbospinal neuronopathy. J Neurol Sci 1993;117:74–78.
18. Schmidt BJ, Greenberg CR, Allingham-Hawkins DJ, Spriggs EL. Expression of X-linked bulbospinal muscular atrophy (Kennedy disease) in two homozygous women. Neurology 2002;59:770–772.
19. Takeyama K, Ito S, Yamamoto A, et al. Androgen-dependent neurodegeneration by polyglutamine-expanded human androgen receptor in Drosophila. Neuron 2002;35:855–864.
20. Chevalier-Larsen ES, O'Brien CJ, Wang H, et al. Castration restores function and neurofilament alterations of aged symptomatic males in a transgenic mouse model of spinal and bulbar muscular atrophy. J Neurosci 2004;24:4778–4786.
21. Shimohata T, Kimura T, Nishizawa M, et al. Five year follow up of a patient with spinal and bulbar muscular atrophy treated with leuprorelin. J Neurol Neurosurg Psychiatry 2004;75: 1206–1207.
22. Norris FH Jr, Calanchini PR, Fallat RJ, et al. The administration of guanidine in amyotrophic lateral sclerosis. Neurology 1974;24:721–728.
23. Trottier Y, Lutz Y, Stevanin G, et al. Polyglutamine expansion as a pathological epitope in Huntington's disease and four dominant cerebellar ataxias. Nature 1995;378:403–406.
24. Terao S, Sobue G, Hashizume Y, et al. Age-related changes in human spinal ventral horn cells with special reference to the loss of small neurons in the intermediate zone: a quantitative analysis. Acta Neuropathol (Berl) 1996;92:109–114.
25. DiFiglia M, Sapp E, Chase KO, et al. Aggregation of huntingtin in neuronal intranuclear inclusions and dystrophic neurites in brain. Science 1997;277:1990–1993.
26. Hayashi Y, Kakita A, Yamada M, et al. Hereditary dentatorubral-pallidoluysian atrophy: ubiquitinated filamentous inclusions in the cerebellar dentate nucleus neurons. Acta Neuropathol (Berl) 1998;95:479–482.
27. Paulson HL, Perez MK, Trottier Y, et al. Intranuclear inclusions of expanded polyglutamine protein in spinocerebellar ataxia type 3. Neuron 1997;19:333–344.
28. Biomarkers Definitions Working Group. Biomarkers and surrogate endpoints: preferred definitions and conceptual framework. Clin Pharmacol Ther 2001;69:89–95.
29. Fleming TR, DeMets DL. Surrogate end points in clinical trials: are we being misled? Ann Intern Med 1996;125: 605–613.
30. Temple R. Are surrogate markers adequate to assess cardiovascular disease drugs? JAMA 1999;282:790–795.

Neurobiology of Disease

Reversible Disruption of Dynactin 1-Mediated Retrograde Axonal Transport in Polyglutamine-Induced Motor Neuron Degeneration

Masahisa Katsuno, Hiroaki Adachi, Makoto Minamiyama, Masahiro Waza, Keisuke Tokui, Haruhiko Banno, Keisuke Suzuki, Yu Onoda, Fumiaki Tanaka, Manabu Doyu, and Gen Sobue

Department of Neurology, Nagoya University Graduate School of Medicine, Showa-ku, Nagoya 466-8550, Japan

Spinal and bulbar muscular atrophy (SBMA) is a hereditary neurodegenerative disease caused by an expansion of a trinucleotide CAG repeat encoding the polyglutamine tract in the *androgen receptor* (*AR*) gene. To elucidate the pathogenesis of polyglutamine-mediated motor neuron dysfunction, we investigated histopathological and biological alterations in a transgenic mouse model of SBMA carrying human pathogenic AR. In affected mice, neurofilaments and synaptophysin accumulated at the distal motor axon. A similar intramuscular accumulation of neurofilament was detected in the skeletal muscle of SBMA patients. Fluoro-gold labeling and sciatic nerve ligation demonstrated an impaired retrograde axonal transport in the transgenic mice. The mRNA level of dynactin 1, an axon motor for retrograde transport, was significantly reduced in the SBMA mice resulting from pathogenic AR-induced transcriptional dysregulation. These pathological events were observed before the onset of neurological symptoms, but were reversed by castration, which prevents nuclear accumulation of pathogenic AR. Overexpression of dynactin 1 mitigated neuronal toxicity of the pathogenic AR in a cell culture model of SBMA. These observations indicate that polyglutamine-dependent transcriptional dysregulation of dynactin 1 plays a crucial role in the reversible neuronal dysfunction in the early stage of SBMA.

Key words: polyglutamine; spinal and bulbar muscular atrophy; androgen; neurofilament; axonal transport; retrograde; dynactin

Introduction

Spinal and bulbar muscular atrophy (SBMA), or Kennedy's disease, is a hereditary neurodegenerative disease resulting from a loss of bulbar and spinal motor neurons (Kennedy et al., 1968; Sobue et al., 1989). Patients present with muscle atrophy and weakness of proximal limbs associated with bulbar palsy, tongue atrophy and contraction fasciculation (Katsuno et al., 2006). The disease affects exclusively adult males, whereas females carrying the mutant *androgen receptor* (*AR*) are seldom symptomatic (Schmidt et al., 2002). The molecular basis of SBMA is an expansion of a trinucleotide CAG repeat, which encodes the polyglutamine tract in the first exon of the *AR* gene (La Spada et al., 1991). This type of mutation has also been found to cause a variety of neurodegenerative disorders, termed polyglutamine diseases, such as Huntington's disease (HD), several forms of spinocerebellar ataxia, and dentatorubral pallidoluysian atrophy (Gatchel and Zoghbi, 2005). Although expression of the causative gene in each of these diseases is ubiquitous, selective neuronal cell death is observed in disease-specific areas of the CNS, suggesting a common molecular basis for these polyglutamine diseases.

Nuclear accumulation of pathogenic protein containing elongated polyglutamine is a crucial step in the pathophysiology of these diseases, providing an important therapeutic target (Adachi et al., 2005; Banno et al., 2006). The aberrant polyglutamine protein has a propensity to form aggregates in the nucleus and inhibits the function of transcriptional factors and coactivators, resulting in transcriptional perturbation (Cha, 2000; Gatchel and Zoghbi, 2005). In support of this hypothesis, altered expression of a variety of genes has been demonstrated in transgenic mouse models of polyglutamine diseases (Sugars and Rubinsztein, 2003). Although polyglutamine-induced transcriptional dysregulation is likely to be central to the pathogenesis of polyglutamine diseases, it has yet to be elucidated which genes are responsible for the selective neurodegeneration (Gatchel and Zoghbi, 2005).

No treatments have been established for polyglutamine diseases, but the androgen blockade therapy, surgical or medical castration, has shown striking therapeutic effects in the SBMA transgenic mouse model (Katsuno et al., 2002, 2003; Chevalier-Larsen et al., 2004). Androgen deprivation strongly inhibits the ligand-dependent nuclear accumulation of pathogenic AR protein, resulting in a striking improvement in neurological and histopathological findings of male mice.

In the present study, we investigated the molecular pathophysiology of motor neuron dysfunction in a transgenic mouse

Received July 18, 2006; revised Sept. 21, 2006; accepted Oct. 6, 2006.

This work was supported by a Center of Excellence grant from the Ministry of Education, Culture, Sports, Science and Technology, Japan, and by grants from the Ministry of Health, Labor and Welfare, Japan. We have no financial conflict of interest that might be construed to influence the results or interpretation of this manuscript. We thank Jun-ichi Miyazaki for kindly providing the pCAGGS vector.

Correspondence should be addressed to Dr. Gen Sobue, Department of Neurology, Nagoya University Graduate School of Medicine, 65 Tsurumai-cho, Showa-ku, Nagoya 466-8550, Japan. E-mail: sobueg@med.nagoya-u.ac.jp.

DOI:10.1523/JNEUROSCI.3032-06.2006

Copyright © 2006 Society for Neuroscience 0270-6474/06/2612106-12$15.00/0

model of SBMA. Polyglutamine-induced transcriptional dysregulation of the dynactin p150 subunit (dynactin 1), an axonal motor-associated protein, resulted in perturbation of retrograde axonal transport in spinal motor neurons in the early stage of the disease. These processes were reversed by castration, which inhibits nuclear accumulation of pathogenic AR. A defect in axonal trafficking of neurofilaments and synaptic vesicles, the potential molecular basis for the reversible pathogenesis, appears to contribute to the initiation of symptoms, and may account for the selective degeneration of motor neurons in SBMA.

Materials and Methods

Generation and maintenance of transgenic mouse. AR-24Q and AR-97Q mice were generated as described previously (Katsuno et al., 2002). Briefly, the full-length human *AR* fragment harboring 24 or 97 CAGs was subcloned into the *Hind*III site of the pCAGGS vector (Niwa et al., 1991) and microinjected into BDF1-fertilized eggs. Five founders with AR-97Q were obtained. These mouse lines were maintained by backcrossing them to C57BL/6J mice. All symptomatic lines (2–6, 4–6, and 7–8) were examined in the present study. All animal experiments were approved by the Animal Care Committee of the Nagoya University Graduate School of Medicine. Mice were given sterile water *ad libitum*. In the experiments where it was called for, sodium butyrate [a histone deacetylase (HDAC) inhibitor] was administered at a concentration of 4 g/L in distilled water from 5 weeks of age until the end of the analysis, as described previously (Minamiyama et al., 2004).

Neurological testing and castration after onset. Mice were subjected to the Rotarod task (Economex Rotarod; Colombus Instruments, Columbus, OH), and cage activity was measured (AB system; Neuroscience, Tokyo, Japan) as described previously (Katsuno et al., 2002). Gait stride was measured in 50 cm of footsteps, and the maximum value was recorded for each mouse. The onset of motor impairment was determined using weekly rotarod task analyses. Male AR-97Q mice were castrated or sham-operated via the abdominal route under ketamine–xylazine anesthesia (50 mg/kg ketamine and 10 mg/kg xylazine, i.p.) within 1 week after the onset of rotarod impairment.

Immunohistochemistry and immunofluorescent analysis. Ten-micrometer-thick sections were prepared from paraffin-embedded tissues, and immunohistochemistry was performed as described previously (Katsuno et al., 2002). Formalin-fixed tail samples were washed with 70% ethanol and decalcified with 7% formic acid–70% ethanol for 7 d before embedding in paraffin. Sections to be immunostained for dynactin 1, dynein intermediate chain, dynein heavy chain, and dynamitin were first microwaved for 20 min in 50 mM citrate buffer, pH 6.0. Sections to be immunostained for polyglutamine (1C2 antibody) were treated with formic acid for 5 min at room temperature. The following primary antibodies were used: anti-dynactin 1 ($p150^{glued}$, 1:250; BD Transduction, San Diego, CA), anti-dynein intermediate chain (1:500; Millipore, Temecula, CA), anti-dynein heavy chain (1:100; Sigma-Aldrich, St. Louis, MO), anti-dynamitin (1:1000; BD Transduction), anti-polyglutamine, 1C2 (1:10,000; Millipore), antiphosphorylated high molecular weight neurofilament (NF-H) (SMI31, 1:1000; Sternberger Monoclonals, Lutherville, MD), anti-nonphosphorylated NF-H (SMI32, 1:5000; Sternberger Monoclonals), and anti-synaptophysin (1:10,000; Dako, Glostrup, Denmark).

For immunofluorescent analysis of skeletal muscle, mice were deeply anesthetized with ketamine–xylazine and perfused with PBS followed by 4% paraformaldehyde fixative in phosphate buffer, pH 7.4. Gastrocnemius muscles were dissected free, frozen quickly by immersion in cooled acetone and powdered CO_2. Longitudinal, 30 μm, cryostat sections were placed on a silane-coated slide in a drop of 3% disodium EDTA, air dried at room temperature, and fixed in methanol/acetone (50:50 v/v). After blocking with PBS containing 5% goat serum and 1% BSA for 30 min at room temperature, sections were incubated with 5 μg/ml Oregon green-conjugated α-bungarotoxin (Invitrogen, Eugene, OR) for 60 min at room temperature. Sections were incubated with antiphosphorylated NF-H (SMI31, 1:5000; Sternberger Monoclonals), anti-synaptophysin (1:50,000; Dako), or anti-Rab3A (1:5000; BD Transduction) antibodies at 4°C overnight, and then with Alexa-546-conjugated goat anti-mouse IgG (1:1000; Invitrogen). Sections were examined with an IX71 inverted microscope (Olympus, Tokyo, Japan). For double staining of the skeletal muscle, paraffin-embedded sections were treated with TNB blocking buffer (PerkinElmer, Boston, MA) and incubated with anti-AR antibody (N-20, 1:500; Santa Cruz Biotechnology, Santa Cruz, CA) together with antiphospho-NF-H.

For immunostaining of human tissues, autopsy specimens of lumbar spinal cord and intercostal muscle obtained from a genetically diagnosed SBMA patient (78-year-old male) and those from a neurologically normal patient (75 years old) were used. The collection of tissues and their use for this study were approved by the Ethics Committee of Nagoya University Graduate School of Medicine. Spinal cord sections at 10 μm were incubated with anti-dynactin 1 antibody ($p150^{glued}$, 1:250; BD Transduction). Thirty-micrometer-thick cryostat sections of intercostal muscle were incubated with 150 μg/ml Alexa-488-conjugated α-bungarotoxin (Invitrogen) and then with antiphosphorylated NF-H (SMI31, 1:200; Sternberger Monoclonals).

Retrograde Fluoro-gold neurotracer labeling. For labeling neurons with intramuscular injection of tracer, mice were anesthetized with ketamine–xylazine, and a small incision was made in the skin of the left calf to expose the gastrocnemius muscle. A total volume of 4.5 μl of 2.5% Fluoro-gold solution (Biotium, Hayward, CA) in PBS was injected in three different parts of the muscle (proximal, middle, and distal) using a 10 μl Hamilton syringe. For labeling by the nerve stump method, the sciatic nerve was exposed and transected at mid-thigh level. A small polyethylene tube containing 2.5% Fluoro-gold solution was applied to the proximal stump of the cut sciatic nerve, and sealed with Vaseline to prevent leakage. Mice were anesthetized 44 h after Fluoro-gold administration with ketamine–xylazine and perfused with PBS followed by 4% paraformaldehyde in phosphate buffer, pH 7.4. Spinal cords were removed and postfixed with 4% paraformaldehyde in phosphate buffer for 2 h, floated in 10 and 15% sucrose for 4 h each and in 20% sucrose overnight. The samples were sectioned longitudinally on a cryostat at 30 μm and mounted on silane-coated slides. The number of Fluoro-gold labeled motor neurons was counted in serial spinal cord sections with an IX71 inverted microscope (Olympus) using a wide-band UV filter. Some specimens were immunostained for dynactin immediately after the number of Fluoro-gold-labeled motor neurons was counted.

Western blot analysis. SH-SY5Y cells were lysed in CellLytic lysis buffer (Sigma-Aldrich) containing a protease inhibitor mixture (Roche, Mannheim, Germany) 2 d after transfection. Mice were killed under ketamine–xylazine anesthesia. Their tissues were snap-frozen with powdered CO_2 in acetone and homogenized in 50 mM Tris, pH 8.0, 150 mM NaCl, 1% NP-40, 0.5% deoxycholate, 0.1% SDS, and 1 mM 2-mercaptoethanol containing 1 mM PMSF and 6 μg/ml aprotinine and then centrifuged at 2500 × *g* for 15 min at 4°C. The supernatant fractions were separated on 5–20% SDS-PAGE gels (10 μg protein for the nerve roots or 40 μg for the spinal cord, per lane) and then transferred to Hybond-P membranes (Amersham Pharmacia Biotech, Buckinghamshire, UK), using 25 mM Tris, 192 mM glycine, 0.1% SDS, and 10% methanol as transfer buffer. Immunoblotting was performed using the following primary antibodies: anti-dynactin 1 ($p150^{glued}$, 1:250; BD Transduction), anti-dynein intermediate chain (1:1000; Millipore), anti-dynein heavy chain (1:200; Sigma-Aldrich), anti-dynamitin (1:250; BD Transduction), anti-α-tubulin (1:5000; Sigma-Aldrich), antiphosphorylated NF-H (SMI31, 1:100,000; Sternberger Monoclonals), and anti-nonphosphorylated NF-H (SMI32, 1:1000; Sternberger Monoclonals). The immunoblots were digitalized (LAS-3000 imaging system; Fujifilm, Tokyo, Japan), signal intensities of three independent blots were quantified with Image Gauge software version 4.22 (Fujifilm), and the means ± SD were expressed in arbitrary units.

Ligation of mouse sciatic nerve. Under anesthesia with ketamine–xylazine, the skin of the right lower limb was incised. The right sciatic nerve was exposed and ligated at mid-thigh level using surgical thread. For immunofluorescent analysis, operated mice were decapitated under deep anesthesia with ketamine–xylazine 8 h after ligation and perfused with 4% paraformaldehyde fixative in phosphate buffer, pH 7.4. The right sciatic nerve segment, including at least 5 mm both proximal and distal to

the ligated site, was removed. The nonligated, left sciatic nerve was also taken out in the same manner as the right nerve. The removed nerves were placed into fixative for 4 h, transferred consecutively to 10, 15, and 20% sucrose in 0.01 M PBS, pH 7.4, for 4 h each at 4°C, mounted in Tissue-Tek OCT compound (Sakura, Tokyo, Japan), and frozen with powdered CO_2 in acetone. Ten-micrometer-thick cryostat sections were prepared from the frozen tissues, blocked with normal goat serum (1:20), incubated with anti-synaptophysin (1:50,000; Dako) at 4°C overnight, and then with Alexa-546-conjugated goat anti-mouse IgG (1:1000; Invitrogen). Immunofluorescent images were recorded with an IX71 inverted microscope (Olympus), and the signal intensities were quantified using Image Gauge software, version 4.22 (Fujifilm) and expressed in arbitrary units.

For immunoblotting of axonal proteins, the sciatic nerve segments 1 mm both proximal and distal to the ligated site were removed without paraformaldehyde fixation, and frozen in with powdered CO_2 in acetone. Protein extraction and Western blotting were performed as described above.

In situ *hybridization*. Formalin-fixed, paraffin-embedded 6-μm-thick sections of the spinal cord were deparaffinized, treated with proteinase K, and processed for *in situ* hybridization using an ISHR kit (Nippon Gene, Tokyo, Japan) according to the manufacturer's instructions. Dynactin 1 cDNA was obtained from spinal cords of wild-type mice. The primers, 5′-AGATGGTGGAGATGCTGACC-3′ and 5′-GAGCCTTGGTCTCAGCAAAC-3′, were phosphorylated with T4polynucleotide kinase (Stratagene Cloning Systems, La Jolla, CA). The cDNA was inserted into the pSPT 19 vector (Roche). Dioxigenin-labeled cRNA antisense and sense probes, 380 bp long, were generated from this plasmid using T7 and SP6 polymerase (Roche), respectively. Spinal cord sections were hybridized for 16 h at 42°C washed in formamide–4× SSC (50:50 v/v) at the same temperature, treated with RNase A at 37°C, and washed again in 0.1× SSC at 42°C. The signals were detected immunologically with alkaline phosphatase-conjugated anti-dioxigenin antibody and incubated with NBT/BCIP (Roche) for 16 h at 42°C. Slices were counterstained with methyl green. To quantify the intensity of the signals in the cell bodies of spinal motor neurons, three nonconsecutive sections from a wild-type littermate and those of a transgenic mouse from lines 7–8 or 4–6 were analyzed using the NIH Image program (version 1.62). Sections adjacent to those used for *in situ* hybridization were processed for immunohistochemistry using anti-polyglutamine antibody as described above.

Quantitative real-time PCR. Dynactin 1 mRNA levels were determined by real-time PCR as described before (Ishigaki et al., 2002; Ando et al., 2003). Briefly, total RNA (5 μg each) from AR-97Q and wild-type spinal cord were reverse transcribed into first-strand cDNA using SuperScript II reverse transcriptase (Invitrogen). Real-time PCR was performed in a total volume of 50 μl, containing 25 μl of 2× QuantiTect SYBR Green PCR Master Mix and 0.4 μM of each primer (Qiagen, Valencia, CA), and the product was detected by the iCycler system (Bio-Rad Laboratories, Hercules, CA). The reaction conditions were 95°C for 15 min and then 45 cycles of 15 s at 95°C followed by 60 s at 55°C. For an internal standard control, the expression level of glyceraldehyde-3-phosphate dehydrogenase (GAPDH) was simultaneously quantified. The following primers used were 5′-CTCAGAGGAGCCCAGATGA-3′ and 5′-GCTGGTCTTGCGGTACAGT-3′ for dynactin 1, 5′-GAGAGCATGGAGCTGGTGTA-3′ and 5′-CCAACCACGAAGTTGTTGAC-3′ for dynein intermediate chain, 5′-TACCAGGTGGGAGTGCATTA-3′ and 5′-CAGTCACTATGCCCATGACC-3′ for dynein heavy chain, 5′-ACAAGCGTGGAACACATCAT-3′ and 5′-TCTTTCCAATGCGATCTGAG-3′ for dynamitin, and 5′-CCTGGAGAAACCTGCCAAGTAT-3′ and 5′-TGAAGTCGCAGGAGACAACCT-3′ for GAPDH. The threshold cycle of each gene was determined as the number of PCR cycles at which the increase in reporter fluorescence was 10 times the baseline signal. The weight of the gene contained in each sample was equal to the log of the starting quantity and the standardized expression level in each mouse was equal to the weight ratio of each gene to that of GAPDH.

For the real-time PCR with mRNA extracted from SH-SY5Y cells, the following primers were used: 5′-CTTGGAAGCGATGAATGAGA-3′ and 5′-TAGTCTGCAACGTCTCCTG-3′ for dynactin 1, and 5′-AGCCTCAAGATCATCAGCAAT-3′ and 5′-GGACTGTGGTCATGAGTCCTT-3′ for GAPDH.

Plasmid vectors and cell culture. Human AR cDNAs containing 24 or 97 CAG repeats were subcloned into pcDNA3.1 (Invitrogen) as described previously (Kobayashi et al., 2000). Human dynactin 1 cDNA was also subcloned into pcDNA3.1 (Invitrogen). The human neuroblastoma cells (SH-SY5Y, #CRL-2266; American Type Culture Collection, Manassas, VA) were plated in 6-well dishes in 2 ml of DMEM/F12 containing 10% fetal bovine serum with penicillin and streptomycin, and each dish was transfected with 2 μg of the vector containing AR24, AR97, or mock and with 2 μg of the vector containing dynactin 1 or mock using Opti-MEM (Invitrogen) and Lipofectamine 2000 (Invitrogen) and then differentiated in differentiation medium (DMEM/F12 supplemented with 5% fetal calf serum and 10 μM retinoic acid) for 2 d. Two days after transfection, cells were stained with propidium iodide (Invitrogen, Eugene, OR) and mounted in Gelvatol. Quantitative analyses were made from triplicate determinations. Duplicate slides were graded blindly in two independent trials as described previously (Katsuno et al., 2005).

Statistical analyses. We analyzed data using the Kaplan-Meier and log-rank test for survival rate, ANOVA with *post hoc* test (Dunnett) for multiple comparisons, and an unpaired *t test* from Statview software version 5 (Hulinks, Tokyo, Japan).

Results

Accumulation of axonal proteins in distal motor axons of SBMA mouse

To clarify the molecular basis of neuronal dysfunction in SBMA, we analyzed histopathological alterations in the spinal cords of transgenic mice carrying full-length human *AR* with 97 CAGs (AR-97Q mice) (Katsuno et al., 2002, 2003). We first focused on the expression and phosphorylation level of NF-H because affected mice demonstrate axonal atrophy in the ventral nerve root (Katsuno et al., 2002). Although it has been widely accepted that NF-H phosphorylation is a crucial factor determining axon caliber, neither the amounts nor the phosphorylation levels of NF-H in spinal cord or ventral root were decreased in male AR-97Q mice compared with wild-type littermates (supplemental Fig. 1*A–C*, available at www.jneurosci.org as supplemental material). The distribution of NF-H in the anterior horn of AR-97Q mice was also indistinguishable from that of wild-type or AR-24Q mice bearing human AR with a normal polyglutamine length (Fig. 1*A*). However, AR-97Q mice demonstrated a striking accumulation of both phosphorylated and nonphosphorylated NF-H in skeletal muscle, a phenomenon not observed in AR-24Q or wild-types (Fig. 1*A*). Although motor neurons originating in the anterior horn are always affected in SBMA, because the primary motor neurons projecting their axons to the anterior horn are not affected, no accumulation is seen in this region. The damage to motor neurons originating within the anterior horn results in accumulation of NFs in the skeletal muscle, instead of the spinal cord. A similar accumulation of the middle molecular weight NF was also observed (data not shown). To clarify whether this phenomenon is specific to neurofilaments, we performed immunohistochemistry on both spinal cord and muscle with an antibody against synaptophysin, a transmembrane glycoprotein of synaptic vesicles that is also retrogradely transported in axons (Li et al., 1995). In AR-97Q mice, synaptophysin accumulated among the muscle fibers in a pattern similar to that of NF-H, whereas no such accumulation was observed in unaffected mice (Fig. 1*B*).

We then investigated the time course of abnormally accumulated NF in skeletal muscle. Because the onset of motor dysfunction occurs at 9–10 weeks in AR-97Q mice, NF pathology before and after the onset was examined. Anti-NF immunostaining demonstrated that intramuscular NF accumulation was detectable as early as 7 weeks before the onset of muscle weakness in this

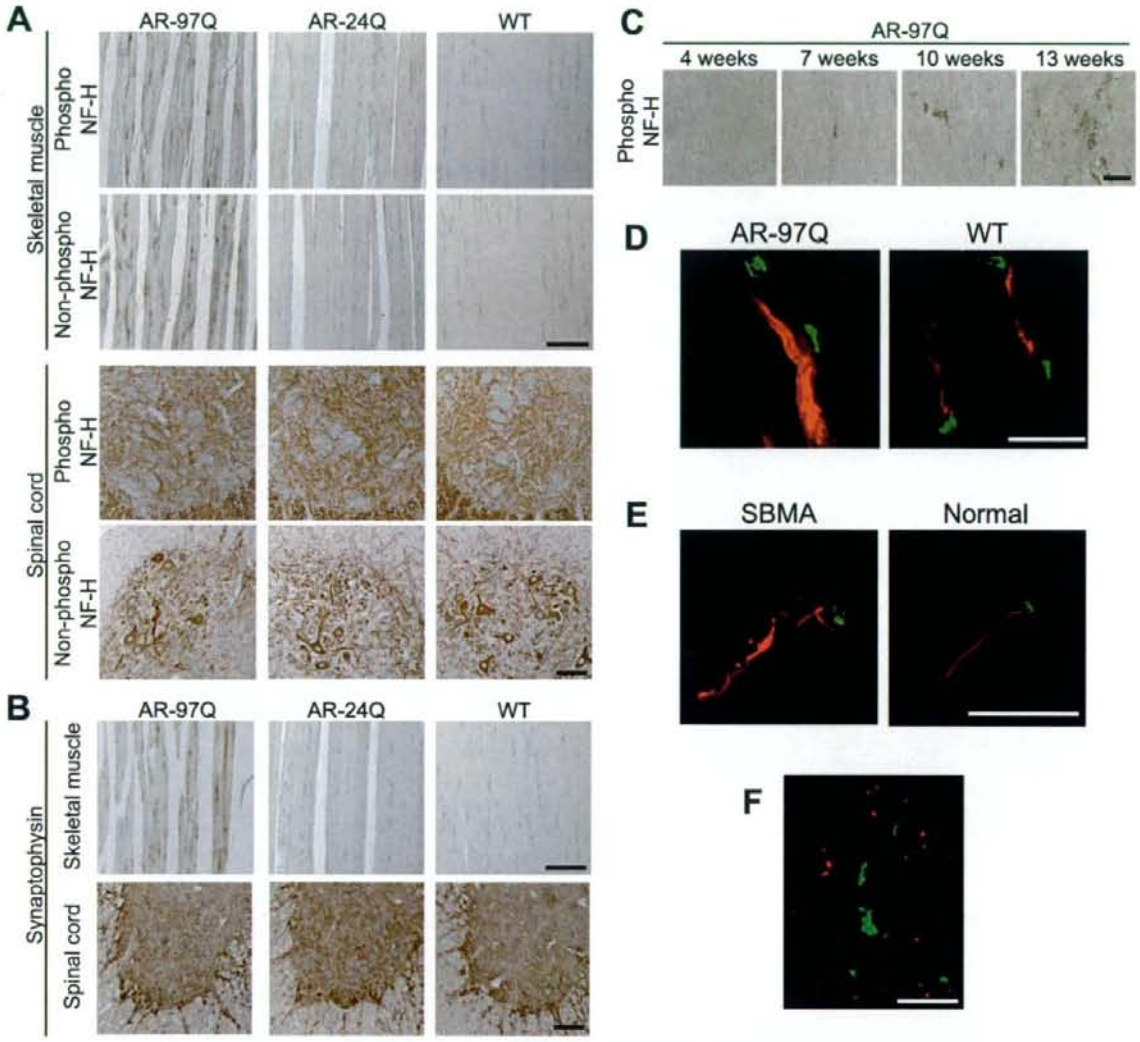

Figure 1. Accumulation of neurofilament and synaptophysin in the distal end of motor axons. ***A***, Immunohistochemistry of skeletal muscle and spinal cord from AR-97Q (4–6), AR-24Q, and wild-type mice (12 weeks) using an antibody for phosphorylated or nonphosphorylated NF-H. ***B***, Immunohistochemistry for synaptophysin shows findings parallel to those of neurofilament. ***C***, Age-dependent change in antiphosphorylated NF-H immunohistochemistry in skeletal muscle of SBMA mice. ***D***, Immunofluorescence of mouse skeletal muscle using α-bungarotoxin (green) in combination with antiphospho-NF-H antibody (red). Phosphorylated NF-H accumulates in the distal end of motor axons in AR-97 mice (7–8, 12 weeks). ***E***, Antiphospho-NF-H immunofluorescence with α-bungarotoxin staining in skeletal muscle from a human SBMA patient showing similar neurofilament accumulation. ***F***, Double-labeling of skeletal muscle from an AR-97Q mouse (4–6, 12 weeks) using antiphospho-NF-H antibody (green) and anti-AR (red) shows that accumulated NF-H does not colocalize with AR. Scale bars, 100 μm.

mouse model, and aggravated thereafter (Fig. 1*C*). These observations suggest that intramuscular accumulation of NF plays a role in the motor neuron dysfunction in this mouse model of SBMA.

To confirm the distribution of NF-H and synaptophysin in skeletal muscle, we examined the localization of these proteins in relation to the neuromuscular junction. Immunohistochemistry using α-bungarotoxin to mark the junctions, and fluorescent-labeled antibodies showed that both NF-H and synaptophysin accumulated in the most distal motor axon adjacent to neuromuscular junctions (Fig. 1*D*). A similar intramuscular accumulation of neurofilament was detected in the skeletal muscle of SBMA patients (Fig. 1*E*). Although pathogenic AR accumulated in the nuclei of skeletal muscle in the AR-97Q mice, the accumulation of NF-H did not colocalize with AR (Fig. 1*F*). Moreover, immunoprecipitation demonstrated no interaction between AR and NF-H (data not shown). These findings exclude the possibility that pathogenic AR directly interrupts the axonal trafficking.

Retrograde axonal transport is disrupted in SBMA mouse

To elucidate the molecular basis of the abnormal distribution of NF and synaptophysin, we studied axonal transport in this mouse model of SBMA. Axonal components undergo anterograde and/or retrograde axonal transport. Proteins including NF and synaptophysin are bidirectionally transported, whereas some

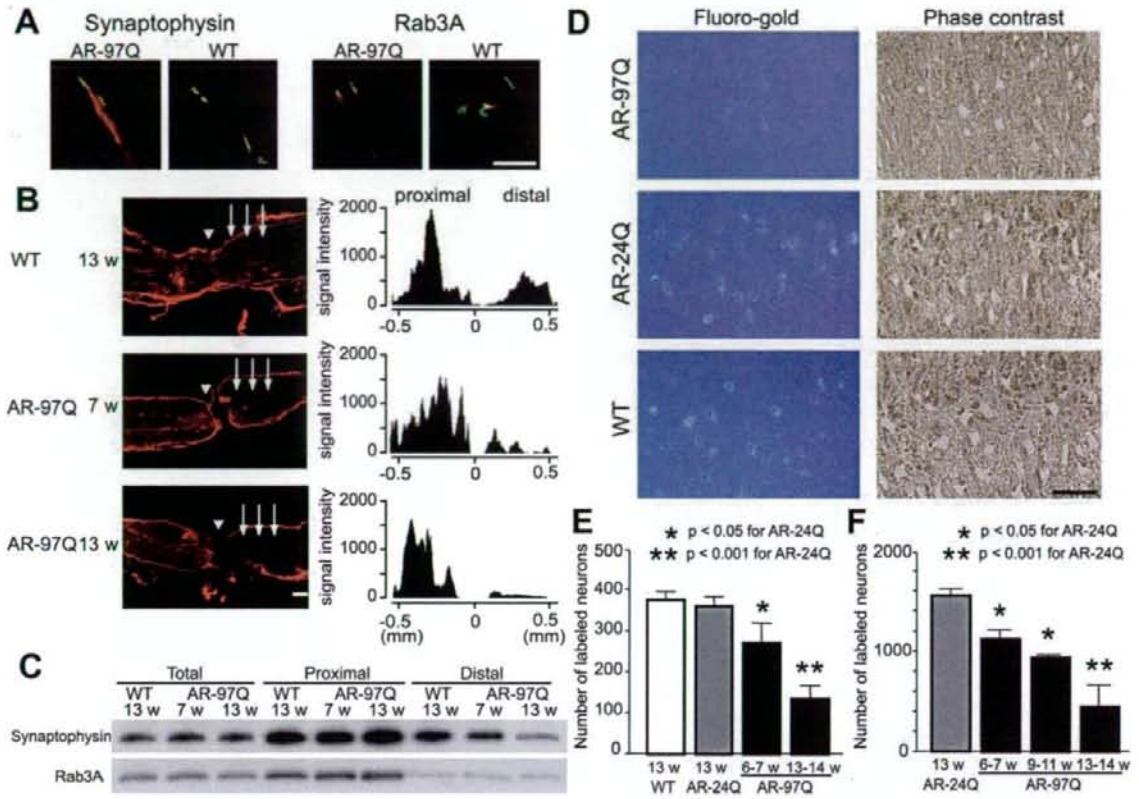

Figure 2. Perturbation of retrograde axonal transport in SBMA mice. ***A***, Immunofluorescence of mouse skeletal muscle using α-bungarotoxin (green) labeling the endplate together with anti-synaptophysin antibody (red) or anti-Rab3A antibody (red). Accumulation of Rab3A is not detected in wild-type or AR-97Q mice (7–8, 12 weeks). ***B***, Immunohistochemistry for synaptophysin in the sciatic nerve 8 h after ligation and representative quantification of immunoreactivity. Accumulation of synaptophysin immunoreactivity is decreased on the distal side (arrows) of the ligation site (arrowhead) in preonset (7 weeks) and advanced stage (13 weeks) AR-97Q mice. ***C***, Immunoblots of the sciatic nerve segments on both proximal and distal sides of the ligation. The total amount of proteins extracted from the contralateral nonligated sciatic nerve was analyzed as a control. ***D***, ***E***, Retrograde labeling of lumbar motor neurons of AR-97Q (7–8), AR-24Q, or wild-type mice (12 weeks) by Fluoro-gold injection into the gastrocnemius muscle (***D***) and the number of labeled neurons (***E***) ($n = 5$ for each group). ***F***, The number of motor neurons labeled by Fluoro-gold using the sciatic nerve stump method ($n = 5$ for each group). Scale bars: ***A***, ***B***, ***D***, 100 μm. Error bars indicate SD.

components such as Rab3A, a small GTP binding protein, are transported only anterogradely (Li et al., 1995; Roy et al., 2000). The distribution of Rab3A in skeletal muscle of SBMA mice was equivalent to that of wild-type mice, whereas synaptophysin and neurofilaments accumulated in the most distal motor axons of the SBMA mice only (Figs. 1*D*, 2*A*).

To further examine the nature of the axonal transport anomaly in SBMA mice, the sciatic nerve was ligated at mid-thigh level. Because the transport rate of NF is slower than other axonal components, we analyzed the transport of synaptophysin and Rab3A in this ligation study (Fig. 2*B*,*C*). In wild-type mice, synaptophysin accumulated predominantly on the proximal side of the ligation, but also on the distal side. Although synaptophysin and Rab3A accumulations proximal to the site of ligation were notable in both preonset and advanced stages of AR-97Q mice, their accumulation on the distal side was decreased before the onset of symptoms and was progressively inhibited. These findings suggest that disrupted retrograde axonal transport gives rise to the accumulation of axonal proteins in the distal motor axon terminals of SBMA mice before the onset of motor impairment.

To confirm this hypothesis, we analyzed retrograde neuronal labeling with the fluorescent tracer Fluoro-gold after its injection into the mouse calf muscle. The number of Fluoro-gold-labeled spinal motor neurons was significantly less in affected AR-97Q mice compared with AR-24Q or wild-type mice (Fig. 2*D*,*E*). To exclude the possibility that synaptic pathology contributed to diminished uptake of the tracer, we also examined Fluoro-gold labeling using direct application of the tracer into the sciatic nerve stump (Sagot et al., 1998). Again, AR-97Q mice showed fewer motor neurons labeled by Fluoro-gold applied directly to the proximal stump of the sciatic nerve than did the AR-24Q mice (Fig. 2*F*), suggesting that neither synaptic retraction nor disconnection is the basis for disruption of axonal transport. Furthermore, it should be noted that the decrease in the number of labeled neurons preceded the onset of motor symptoms in both of these experiments. These observations suggest that the disruption of retrograde transport plays an early role in the pathogenesis of motor neuron degeneration in SBMA.

Transcriptional dysregulation of dynactin 1 in SBMA

Retrograde axonal transport is microtubule-dependent and is regulated by the axon motor protein dynein and its associated protein complex, dynactin. To elucidate the molecular

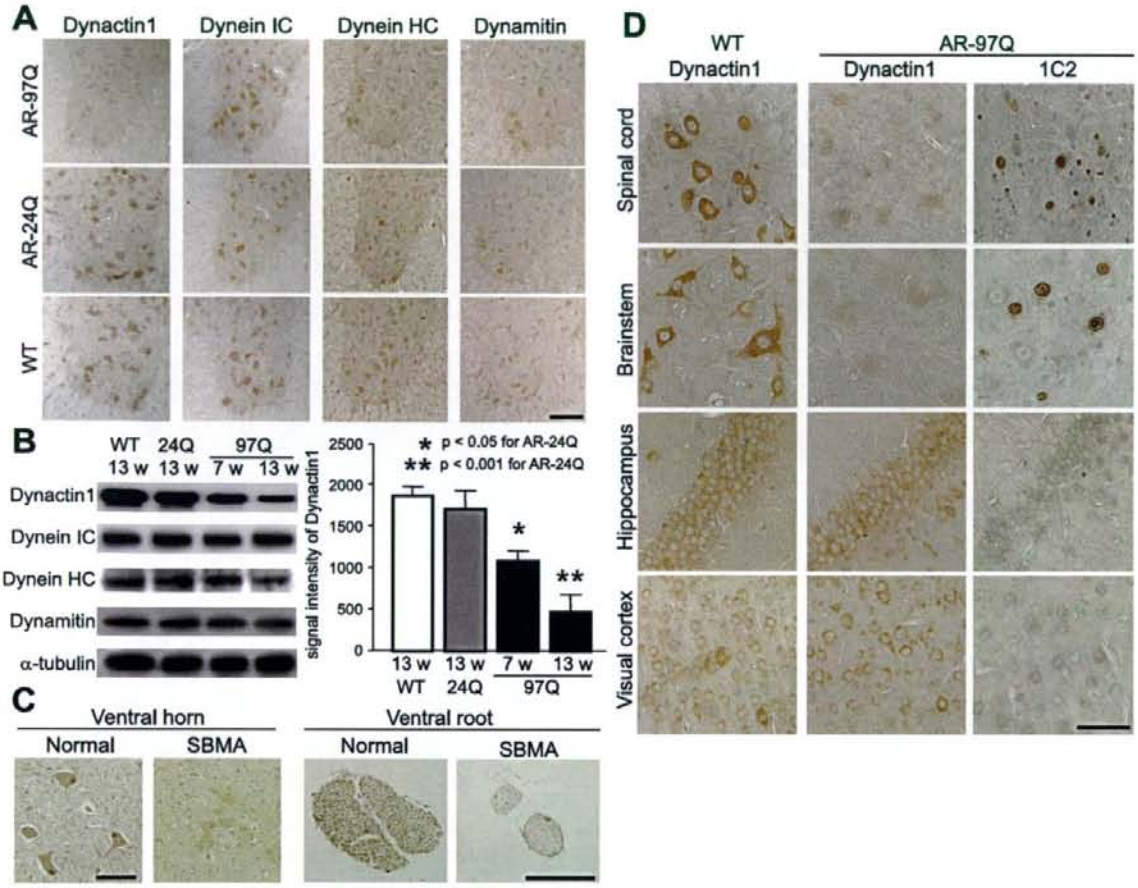

Figure 3. Decreased levels of dynactin 1 in SBMA. ***A***, Immunohistochemistry for motor proteins regulating retrograde axonal transport, dynactin 1, dynein intermediate chain (IC), dynein heavy chain (HC), and dynamitin in the spinal cord from AR-97Q (4–6), AR-24Q, and wild-type mice (12 weeks). Dynactin 1 is markedly diminished in the motor neurons of AR-97Q mice. ***B***, Western blot analysis for motor proteins in the ventral spinal root from presymptomatic or advanced AR-97Q mice (4–6) compared with those from AR-24Q and wild-type mice. ***C***, Dynactin 1 immunohistochemistry in the anterior horn and the ventral root of an SBMA patient and a normal subject. ***D***, Anti-dynactin 1 immunohistochemistry in various affected (spinal cord and brainstem) and nonaffected (hippocampus and visual cortex) tissues from wild-type and AR-97Q mice. Data from AR-97Q mice are compared with immunohistochemistry using the anti-polyglutamine antibody, 1C2. Scale bars: ***A***, 100 μm; ***C***, ***D***, 50 mm. Error bars indicate SD.

mechanism compromising retrograde axonal transport in SBMA mice, we examined the levels of various dynein and dynactin protein subunits. Immunohistochemistry of spinal cord sections demonstrated that the spinal motor neurons from AR-97Q mice had lower levels of dynactin 1, the largest subunit of dynactin, than did those from either wild-type or AR-24Q mice (Fig. 3*A*). In the ventral root, significantly decreased levels of dynactin 1 were apparent before the onset of motor symptoms (Fig. 3*B*). Although the level of dynein heavy chain was diminished in the advanced disease stage in SBMA mice, this phenomenon was not observed before the onset of symptoms (Fig. 3*B*). No alterations were observed in the levels of dynein intermediate chain or dynamitin, the p50 subunit of dynactin, throughout the disease course (Fig. 3*A*, *B*). To confirm the role of dynactin 1 in the pathogenesis of human SBMA, we also examined the protein level in autopsy specimens. As observed in the mouse model, the protein level of dynactin 1 was decreased in the anterior horn cells and in the ventral roots of SBMA patients (Fig. 3*C*).

To examine the cell specificity of reduced dynactin 1 levels we compared anti-dynactin 1 immunohistochemistry with that of anti-polyglutamine using the 1C2 antibody in various tissues from wild-type and AR-97Q mice (Fig. 3*D*). The immunoreactivity of dynactin 1 was markedly diminished in 1C2-positive tissues, but not in those lacking nuclear polyglutamine staining. This observation suggests that the reduction in dynactin 1 is relevant to the polyglutamine-mediated neuropathology. In addition, to investigate whether reduced levels of dynactin 1 were correlated with defective retrograde axonal transport, we analyzed anti-dynactin 1 immunohistochemistry in spinal cord sections labeled by Fluoro-gold (supplemental Fig. 2, available at www.jneurosci.org as supplemental material). The levels of dynactin 1 were decreased in the spinal motor neurons of AR-97Q mice concomitantly with decreased intensities of Fluoro-gold labeling. Together, these data strongly suggest that depletion of dynactin 1 is responsible for the disruption of retrograde axonal transport in SBMA.

To clarify the pathological mechanism responsible for reduc-